

Synthesis and Chirality of Amino Acids Under Interstellar Conditions

Chaitanya Giri, Fred Goesmann, Cornelia Meinert, Amanda C. Evans, and Uwe J. Meierhenrich

Please note the erratum to this chapter at the end of the book.

Abstract Amino acids are the fundamental building blocks of proteins, the biomolecules that provide cellular structure and function in all living organisms. A majority of amino acids utilized within living systems possess pre-specified orientation geometry (chirality); however the original source for this specific orientation remains uncertain. In order to trace the chemical evolution of life, an appreciation of the synthetic and evolutionary origins of the first chiral amino acids must first be gained. Given that the amino acids in our universe are likely to have been synthesized in molecular clouds in interstellar space, it is necessary to understand where and how the first synthesis might have occurred. The asymmetry of the original amino acid synthesis was probably the result of exposure to chiral photons in the form of circularly polarized light (CPL), which has been detected in interstellar molecular clouds. This chirality transfer event, from photons to amino acids, has been successfully recreated experimentally and is likely a combination of both asymmetric synthesis and enantioselective photolysis. A series of innovative

C. Giri

Max Planck Institute for Solar System Research, Max-Planck-Str. 2, 37191 Katlenburg-Lindau, Germany

Institut de Chimie de Nice, University of Nice-Sophia Antipolis, UMR 7272 CNRS, 28 Avenue Valrose, 06108 Nice Cedex 2, France

F. Goesmann

Max Planck Institute for Solar System Research, Max-Planck-Str. 2, 37191 Katlenburg-Lindau, Germany

C. Meinert and U.J. Meierhenrich (✉)

Institut de Chimie de Nice, University of Nice-Sophia Antipolis, UMR 7272 CNRS, 28 Avenue Valrose, 06108 Nice Cedex 2, France

e-mail: Uwe.Meierhenrich@unice.fr

A.C. Evans

Institut de Chimie de Nice, University of Nice-Sophia Antipolis, UMR 7272 CNRS, 28 Avenue Valrose, 06108 Nice Cedex 2, France

University of Cambridge, Murray Edwards College, Cambridge CB3 0DF, UK

studies have reported successful simulation of these environments and afforded production of chiral amino acids under realistic circumstellar and interstellar conditions: irradiation of interstellar ice analogues (CO, CO₂, NH₃, CH₃OH, and H₂O) with circularly polarized ultraviolet photons at low temperatures does result in enantiomer enriched amino acid structures (up to 1.3% ee). This topical review summarizes current knowledge and recent discoveries about the simulated interstellar environments within which amino acids were probably formed. A synopsis of the COSAC experiment onboard the ESA cometary mission ROSETTA concludes this review: the ROSETTA mission will soft-land on the nucleus of the comet 67P/Churyumov-Gerasimenko in November 2014, anticipating the first in situ detection of asymmetric organic molecules in cometary ices.

Keywords Amino acids · Chirality · Churyumov-Gerasimenko · Circularly polarized radiation · COSAC · GC–MS · Molecular clouds · PHILAE · ROSETTA

Contents

1	Introduction to Interstellar Space	43
1.1	Interstellar Medium	43
1.2	Objects in ISM	44
2	Origin and Abundance of Organics in Interstellar Space	47
2.1	Origin of Carbon–Carbon Stars	47
2.2	Interstellar Dispersion and Abundance of Organic Molecules	49
3	The Requisite for a Substrate: Interstellar Dust	50
3.1	Sources of ISD	50
3.2	Density and Diversity of Molecules	52
3.3	Radiation Dosage on the Icy Grain Mantle Surface	52
3.4	Accretion of Organics on Icy Mantles	56
4	The Formation of Amino Acids and the Origin of Homochirality in Interstellar Space . .	57
4.1	Asymmetry Propagates Asymmetry	57
4.2	The Detection of Amino Acids in Interplanetary Space	60
5	Production of Amino Acids in Laboratory Simulation Experiments	61
5.1	Laboratory Studies on Amino Acid Formation in Interstellar Ice Analogues	61
5.2	Asymmetric Photochemistry and Anisotropy Spectra of Amino Acids	63
5.3	Asymmetric Amplification Processes	65
5.4	The Higher Order Structures of Amino Acids	66
6	The COSAC Experiment on ROSETTA: The First Advances	69
6.1	PHILAE Lander and COSAC	69
6.2	The Scientific Vision of COSAC	73
7	Outlook	75
	References	76

Abbreviations

Amu	Atomic mass unit
AU	Astronomical unit
A _v	Total visual extinction
DMF–DMA	Dimethylformamide–dimethylacetal

ECEE	<i>N,N</i> -ethoxycarbonyl ethyl ester
Kpc	Distance in kiloparsecs
$M_{\odot} \text{ pc}^{-2} \text{ Gyr}^{-1}$	Mass loss rate per square parsec per gigayear
$M_{\odot} \text{ yr}^{-1}$	Mass loss rate
$n(\text{H}_2) \text{ yr}$	Accretion rate of hydrogen molecule
n_{H}	Condensate density
NIR	Near infrared
pcs	Parsecs
UV	Ultraviolet

1 Introduction to Interstellar Space

The universe is a boundless expanse inclusive of matter, energy, and the physical entities embodying them: cosmic dust, molecular clouds, stars, planets, nebulae, and the physicochemical signaling and self-replicating process known as life.

In terms of vastness of celestial bodies, galaxies are colossal clusters of millions of stars and their associated planets, asteroids, comets, icy bodies, and interstellar media (ISM). It is difficult to comprehend simultaneously every phenomenon concurrently occurring within such vast galactic systems. The interstellar medium (ISM) within a galaxy is defined as the portion of the galaxy where no stars and planets exist apart from matter and cosmic radiation. The chemistry that occurs in interstellar regions of different galaxies, and even within the same galaxy, can be highly diverse due to the variety of different environments in terms of the densities, temperatures, and masses of the systems involved. In this topical review we will focus on the ongoing interstellar chemistry towards the formation of prebiotic molecules, the origins of their stereochemistry, and thus the potential molecular origins of today's homochiral evolving life systems.

1.1 Interstellar Medium

A star system identical to our solar system would include a star, planets revolving around it in their orbits, asteroids, interplanetary dust, and icy bodies. Beyond the sphere of influence of any star, known as the heliosphere, exists the ISM. The term “interstellar” refers to any object occupying the space that exists between two or more stars. The interstellar boundary of our solar system is a region within the heliosphere where solar wind speeds decline from supersonic to subsonic levels due to an interfacing with the immediate ISM – this phenomenon is called termination shock [1]. Interstellar space exists beyond this termination shock. The ISM is consequently indigenous and beyond the physical influence of the heliosphere.

The ISM is primarily composed of particulate dust, hydrogen, helium, and heavier elements which are present in ionized, non-ionized, molecular gaseous

Table 1 Elemental abundance in interstellar medium [4]

Elements	Abundance by number (%)	Abundance by mass (%)
Hydrogen	90.8	70.4
Helium	9.18	28.1
Heavier elements (metals)	0.12	1.5

Table 2 Temperature-density values of neutral medium [2]

Medium	Temperature (K)	Density (cm^{-3})
WNM	8,000	0.5
CNM	80	50

phases or in solid-states [2]. The density of these various states ranges from $\sim 1.5 \times 10^{-26} \text{ g/cm}^3$ in hot medium to $\sim 2 \times 10^{-19} \text{ g/cm}^3$ in dense molecular clouds [3]. The elemental composition of the ISM is comparable to the cosmic elemental composition; this is contingent upon the abundance measurements of these elements in disk-like stars, sun, and meteorites. Hydrogen is the most abundant element in the ISM followed by helium and other heavier elements (Table 1) [4].

One possible justification for the low abundances of heavier elements seen to be present in the ISM can be inferred from the interstellar absorption lines observed in the far-ultraviolet spectra of hot stars. A large fraction of heavier elements are depleted from the ISM but might be captured and accumulated by the interstellar dust (ISD) grains [5]. Commonly detected Period Two elements like C, O, and N have been observed to be depleted by an average factor of ~ 1.2 –3, while heavier elements resistant to very high temperatures, such as Fe, Si, and Mg, are depleted by an average factor of ~ 10 –100 from the ISM. These observations indicated that although ISD comprises 0.5–1% of the total interstellar mass, it could well play a pivotal role in dictating the dynamic chemical composition of the ISM [6].

1.2 Objects in ISM

The majority of the ISM exists in the gaseous phase. Various gases tend to accumulate within regions of ISM as ionized, neutral, or molecular clouds, depending on their constituent expanse, temperature, and density (Table 2). Hydrogen, the most abundant element in the universe, is found in gaseous neutral state, gaseous ionized state, or in molecular gaseous form within these clouds. The objects/clouds formed from each of these three compositions respectively are known as H I cloud regions, H II cloud regions, and molecular clouds. The H I and H II cloud regions are also referred to as diffuse clouds, while molecular clouds are also known as dense clouds.

1.2.1 H I Regions

Due to the low density of hydrogen in some regions of ISM, particle collision frequency is correspondingly low; hence most hydrogen atoms in these low density regions exist in ground state electronic level, $n = 1$. These low density regions are called H I cloud regions. It is difficult to observe H I regions at visual light wavelengths but it is relatively easy to observe them in the UV and it is also possible to visualize characteristic optical absorption lines of metallic elements in the field of view of bright background stars. The neutral hydrogen extant in H I regions is commonly observed by radio telescopes using an H 21 cm absorption line. Temperature and density are interdependent in these H I regions (Table 2) and are observed in the form of both the diffuse cold neutral medium (CNM) and the less dense warm neutral medium (WNM) [2].

1.2.2 H II Regions

In these larger, low-density cloud regions the formation of massive and extremely luminous stars, being bluish in appearance, has recently occurred. The so-called O-type and B-type main sequence stars are the largest and hottest of this type of luminous stars known to exist in the Milky Way Galaxy. These blue giants emit highly energetic UV radiation below 912 Å (corresponding to an energy input of 13.6 eV) that is strong enough to ionize neutral gases such as hydrogen. The hydrogen atoms in these H II regions are therefore almost fully ionized but their thermal electrons and protons readily recombine and are then reionized by the emitted UV radiation. The degree of hydrogen ionization remaining in equilibrium state in these regions is affected by variations in UV ionization and subsequent recombination. Any superfluous radiation that is not used by the system for ionization is then converted by thermally-excited electrons into kinetic energy. The density of H II cloud regions ranges between 1 and 10^5 atoms/cm³ and the temperature is 10^4 K: thus these regions are denser and thermally more active than the H I regions [3]. H II regions exhibit diverse morphologies from filamentous (e.g., Cygnus nebula) to clump-like (e.g., Carina nebula, Fig. 1), owing to large density gradients within their structures.

1.2.3 Molecular Clouds

Molecular clouds are large dense clouds within which a variety of molecules are known to be generated, particularly molecular hydrogen (H₂). Shock waves due to supernovae, collisions between clouds, and magnetic interactions can all trigger the collapse of portions of the molecular cloud and subsequently lead to star formation. It is difficult to probe the dense dusty interiors of these molecular clouds using optical and UV absorption lines. Radio waves provide an alternative method for

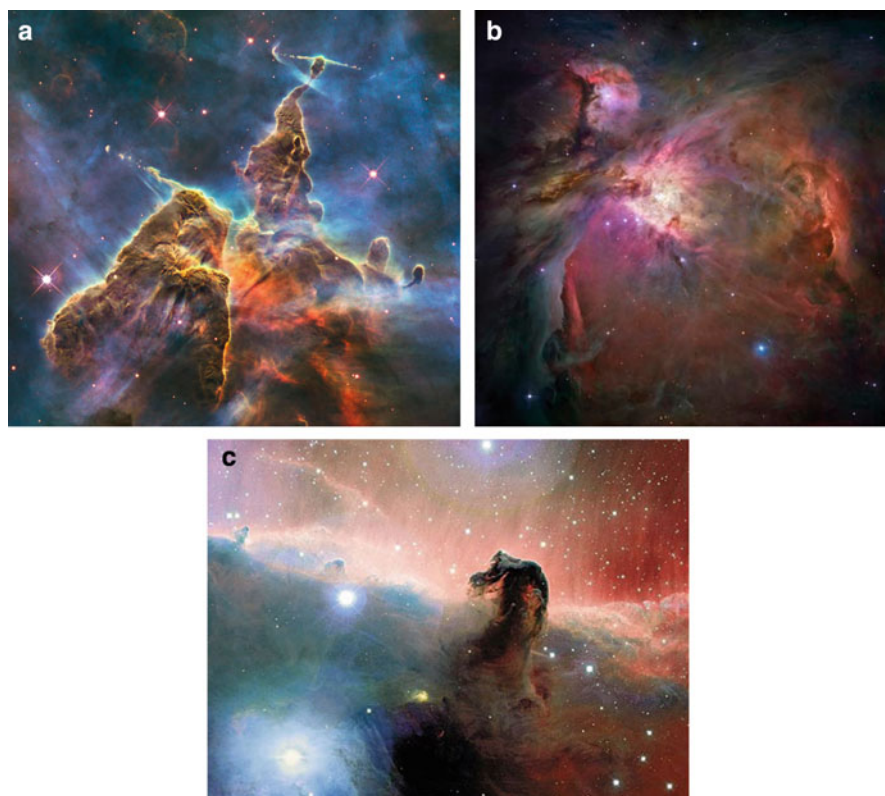


Fig. 1 (a) Optical image of a stellar nursery pillar from Carina Nebula taken from the NASA/ESA Hubble's Space Telescope. The Carina Nebula is located 7,500 light years away from Earth in the constellation Carina. The pillar observed above is approximately 3 light years tall and consists of densely packed gases and dust [image credits: NASA, ESA, M. Livio and the Hubble twentieth Anniversary Team (STScI)]. (b) Optical image of the Orion Nebula taken from the NASA/ESA Hubble's Space Telescope. The Orion Nebula is 1,500 light years away from the Earth and is the nearest star formation region to our solar system [image credits: NASA, ESA, M. Robberto (Space Telescope Science Institute/ESA) and the Hubble Space Telescope Orion Treasury Project Team]. (c) Representative-color image of the Horsehead Nebula taken from the Canada–France–Hawaii Telescope (CFHT) in Hawaii. The Horsehead Nebula is entrenched in the enormous Orion Nebula. It is a dark molecular cloud of dust that is particularly visible due to a brighter background creating a silhouette. The distinct horsehead structure is an extension of a large, dark and dusty molecular cloud [image credits: Jean-Charles Cuillandre (CFHT), Hawaiian Starlight, CFHT]

chemically characterizing the contents of these dense cloud regions as they are able to penetrate these dense clouds without extinction. This discovery has led to wide applications of radio spectroscopy in astronomy.

Stable H_2 molecules possess no electric dipole moments and have negligible moments of inertia: their permitted transitions lie outside the radio domain of the electromagnetic spectrum and hence H_2 is not directly observed at radio wavelengths [7]. Another molecule commonly found in these molecular cloud

regions, carbon monoxide (CO), is therefore used by astronomers as a primary tracer molecule for interstellar molecular clouds [8]. CO is easy to trace using radio spectroscopy due to its rotational transition of $J = 1 \rightarrow 0$ at radio wavelengths of 2.6 mm and also possesses a strong electric dipole moment [9]. The dense packing of matter within molecular cloud regions can lead to extensive gas-phase chemistry driven by the cosmic ray ionization that can penetrate within the cloud. Molecular clouds have cooler temperatures (10 K) than H I and H II regions, and this characteristic serves to enhance molecular accretion onto ISD grains and the formation of icy mantles on the surfaces of ISD grains. Such enhanced gas–grain interactions can result in a greater diversity of chemical species that can exist in these clouds.

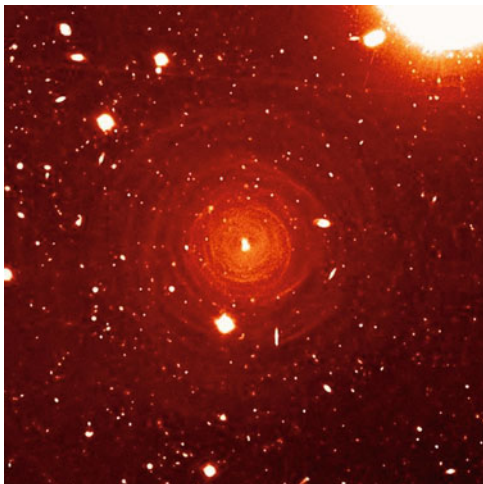
2 Origin and Abundance of Organics in Interstellar Space

Interstellar space contains an abundant collection of dispersed organic compounds. Observations at infrared, radio, millimeter, and sub-millimeter frequencies have detected more than 160 different molecular species in both gas and condensed phases in star-forming regions [10, 11]. These comprise both simple and complex species and stable or transient molecules. In addition to large abundances of H₂ and He, a host of other molecules (nitriles, aldehydes, alcohols, acids, ethers, ketones, amines, amides, long-chain hydrocarbons) have been identified in the ISM. These more complex organic molecules that pervade interstellar clouds constitute an important fraction of the available carbon in the universe. Some of these organics are considered to be fundamental precursor molecules of the basic building blocks for carbon-based cellular life on Earth. However, an understanding of how basic building blocks evolve into the complex self-replicating organic systems remains elusive [12, 13]. Additionally, the events that originally resulted in the exogenous delivery of organic matter to Earth in terms of time and volume have yet to be elucidated.

2.1 *Origin of Carbon–Carbon Stars*

The origin of organic molecules in the universe is directly linked to the origin of carbon in the universe. Carbon is the sixth most abundant element in the universe [14]. The origin of carbon itself can be traced to the fusion reactions that are known to occur within stellar interiors – the products of these fusion reactions are believed to be ejected into far away interstellar space during stellar collapse and supernova bursts. This mechanism is conceivable as it can both generate and disperses stellar material. However, there is another major source of carbon production in the universe – carbon stars.

Fig. 2 Optical image of carbon star IRC +10216 taken from Focal Reducer and low dispersion Spectrograph (FORS1) on the Very Large Telescope of European Space Observatory. The concentric layers around the central star form the dusty astrosphere of IRC +10216. The astrosphere radius is approximately 84,000 AU and is a distinct source of organic molecules and dust [20, 21] (image credits: Izan Leao, Universidade Federal do Rio Grande do Norte, Brazil)



Classical carbon stars are late-type stars similar to red giants. They have a carbon/oxygen (C/O) ratio greater than unity that is characterized by an exceptionally strong C_2 absorption band in addition to CN and CH absorption bands. The high C/O ratio at the surface of these red giants can be due to CNO processing, helium-core flash, or helium shell flash. As carbon stars are main-sequence stars, they eject large quantities of surface matter slowly into space [15].

IRC +10216 is the closest carbon star to Earth: it is located at a distance of 120–250 pcs within the Milky Way Galaxy [16–19] and was first discovered by Eric Becklin and his team while using the Caltech Infrared Telescope at the Mount Wilson Observatory in 1969 (Fig. 2) [18]. The Herschel Space Observatory instrument HIFI has measured a mass loss rate of $4.0 \times 10^{-8} M_{\odot} \text{ yr}^{-1}$ from IRC +10216 [22]. This mass-loss suggests an interesting reason for the observed sooty appearance of the regions surrounding around carbon stars. Within the optically thick and dusty astrosphere of IRC +10216, more than 70 different chemical species have been detected. The Sub-millimeter Wave Astronomy Satellite – a NASA project studying the chemical composition of interstellar gas clouds – has also detected circumstellar water vapor in the astrosphere of IRC +10216. These observed water vapor spectral lines have been detected in a highly excited state, which indicates the presence of much warmer water molecules at temperatures of 1,000 K [23].

Carbon is observed to be the main constituent of ISD grains, which will be discussed in detail in Sect. 3 of this review. In 1969, Gilman suggested that graphite, an allotrope of carbon, should be the first species to condense from low-temperature carbon-rich gas into ISD grains [19]. Once formed, these ISD grains are capable of accreting molecules in the gas phase on their surfaces to form surrounding mantles of organic ices. Numerous dust species of this nature have been detected in the astrosphere of IRC +10216. It is currently thought that these ISD grains might act as reactive surfaces for driving solid phase organic chemistry in interstellar space.

Table 3 Inventory of astrosphere of carbon star IRC +10216

Chemical functional group	Chemical species	References
Cyanopolynes	HC ₃ N, HC ₅ N, HC ₇ N, HC ₉ N, HC ₁₁ N	[25]
Acetylenic compounds	C ₂ H, C ₃ H, C ₄ H, C ₅ H, C ₆ H	[26]
Carbenes	H ₂ CCC, H ₂ CCCC	[27]
Carbon chain molecules	C ₂ , C ₃ , C ₅ , C ₃ N	[28]
Simple organics	HCN, CN, C ₂ H ₂ , CH ₄ , C ₂ H ₄ , CH ₃ CN, HC ₂ N	[21]

2.2 *Interstellar Dispersion and Abundance of Organic Molecules*

Carbon is mainly present in interstellar space in the form of CO, which is commonly used by astronomers as a primary tracer for molecular clouds within the ISM. The next most abundant carbon-containing molecule observed is acetylene. As CO is less reactive and more stable than acetylene, it is generally assumed that complex interstellar organic chemistry usually utilizes acetylene as a primary substrate [24]. The astrosphere of the carbon star IRC +10216 has been propagating at a speed of ≥ 91 km/s over the past 69,000 years and current predictions estimate the radius of its astrosphere to be 84,000 AU [20]. These data suggest that a carbon star could be a dominant source of organic species and possibly possess the ability to disperse these organic species into distant interstellar space in a non-destructive manner (Table 3).

In addition to having been observed in the nebulae formed around carbon stars, organics are observed in the various interstellar cloud structures. These clouds are characterized by their visual extinction into three individual cloud groups: diffuse clouds ($A_V \leq 1$ mag), dense clouds ($A_V > 5$ mag), and translucent clouds ($1 \text{ mag} \leq A_V \leq 5 \text{ mag}$) [29].

As already outlined in Sect. 1.2.3, dense molecular clouds are considered to be the stellar nurseries of the universe and are abundant in both organic molecular species and ISD grains. The density of these clouds results from the gravity exerted by constituent cloud matter that acts inwardly upon the cloud structure. The high density and low temperatures of these molecular clouds assist in promoting molecular synthesis on the ISD grain surfaces.

Dense clouds can be further broken down into three sub-regions in which distinct chemical processes occur [30, 31]. In one type of sub-region, organic molecules are generated within the condensed phase existing on ISD grain substrates. At low temperatures these dust grains thus acquire an icy mantle of molecules that have accreted from the gaseous phase. Interaction with interstellar radiation can activate numerous chemical processes that subsequently yield organic molecules, depending on the energy of the radiation and the system itself [30, 31].

In another type of sub-region of dense molecular clouds, ISD grains tend to shield interior regions that are largely made up of gaseous matter; radiation thus does not reach these gaseous shielded inner regions. However the ISD grains here permit penetration of low intensity cosmic rays that can initiate and drive ion-rich molecular reactions along with neutral molecule processes that are known to result in the formation of a number of organic species [32].

A third typology of dense cloud sub-regions is known as “hot molecular cores” – these are cloud regions of high temperature in which sputtering and evaporation of icy grain mantles have recently occurred [33]. Due to their highly thermodynamic natures, these regions are rich with the synthesis of organic molecules of diverse complexity.

3 The Requisite for a Substrate: Interstellar Dust

Robert J. Trumpler was a prominent Swiss-American astronomer of the early twentieth century. He was interested in observing galactic open clusters – a group of co-evolved stars formed from the same parent molecular cloud. He observed that remote galactic open clusters appear to be roughly twice the size of closer ones. Failing to find an observational inaccuracy he assumed that this size difference could be due to the existence of an unknown absorbing medium extant between the galactic open clusters and the observer on Earth. Trumpler also assumed that the quantity of absorbing medium would increase with distance from the observer, thereby causing more distant open clusters to appear dimmer and resulting in an overestimation of their size and distance. He later calculated that the luminosity of a star is decreased by this absorbing medium by a factor of 1.208 for every 1,000 light-years the starlight travels toward Earth [34]. This absorbing medium that Trumpler postulated was later found to be ISD.

ISD is a fundamental substrate for the synthesis of complex molecules in interstellar space. The low temperatures ($\sim 3\text{--}90\text{ K}$) and densities ($\sim 10^6\text{ H atoms/cm}^3$) observed in dense molecular clouds favor the condensation of volatile molecules from the gas phase onto the surface of ISD grains and thus lead to diverse molecular products. Of these molecular products, the formation of amino acids and the chemical processes involved in their interstellar synthesis are of primary importance for the purposes of this review. Amino acids are the basic building blocks used for the majority of life’s structural and functional processes and are therefore considered to be key prebiotic molecules.

There are a number of important factors necessary for the generation of amino acids onto ISD grain surfaces. These are: (1) the source of ISD; (2) the density and diversity of volatile molecules present in the icy mantle; (3) the radiation dosage to which the icy mantle surface of the ISD grain is exposed; (4) the evolutionary lifespan of the organic icy mantle on the ISD grain.

3.1 Sources of ISD

It is commonly said that “we are all made of stardust.” This statement may be spiritually inspiring but provides very little scope for understanding the origin of ISD in the universe. Stars late in their lives do donate their innate matter into space

Fig. 3 Infrared image of Cassiopeia A taken by Spitzer Space Telescope. The region in *blue* contains matter expelled during the supernova explosion and energized by a forward shock wave; this region is now composed of stars born from this matter (see *blue dots*). The regions of *red*, *green*, and *yellow* contain the same matter which is heated by a reverse shock wave (image credits: NASA/JPL-Caltech/Rudnick L, University of Minnesota, USA)



either tranquilly or destructively, but this material donation does not itself constitute the only source of ISD.

Cosmic dust is a collective term for dust present in interplanetary, interstellar, and intergalactic space. However, the amorphous silicate and carbon-based submicron-sized dust grains in the above three dimensions vary depending on their origin, chemical composition, and morphology. ISD is believed to act as a substrate for a wide variety of gas-grain chemical reactions. It is thus also known to influence the chemical, thermal, and ionization states of matter actively participating in the chemical evolution of the universe. Mass loss from the evolved stars in the asymptotic giant branch (AGB) phase is one of the main sources of ISD grains. These evolved stars of intermediate mass emit dust at a rate of 5.3×10^{-3} to $6.5 \times 10^{-3} M_{\odot} \text{ pc}^{-2} \text{ Gyr}^{-1}$ [35]. The chemical composition of the ISD grains produced depends upon the type of the giant star producing them, and these composition differences are usually observed with reference to C/O ratios. Oxygen rich M-type giants have C/O ratios less than unity, whereas carbon-rich C-type stars have a C/O ratio greater than unity and are thus much more likely to be producing ISD [36]. The carbon-rich Mira type star IRC +10216 has proven itself capable of ejecting carbon-rich dust over quite a long span of time – $4.0 \times 10^{-8} M_{\odot} \text{ yr}^{-1}$ [22]. Such a long, gradual, and non-destructive dust emission process can ensure the transportation of ISD over vast distances ($\sim 84,000$ AU in this instance) [20].

Another common source of ISD is the rapid breakdown and violent explosion of the massive stars known as type II supernovae. Vast amounts of dust, as much as $\sim 2\text{--}4 M_{\odot}$, have been observed in the galactic supernova remnant Cassiopeia A (Fig. 3) and have also been detected using the SCUBA array on the James Clerk Maxwell Telescope in Hawaii. These type II supernovae explosions can contribute significantly to the dust inventory of a galaxy with an estimated dust production rate of $7\text{--}18 \times 10^{-3} M_{\odot} \text{ yr}^{-1}$ [37], relative to stellar production rates of $\sim 5 \times 10^{-3} M_{\odot} \text{ yr}^{-1}$ [38].

3.2 *Density and Diversity of Molecules*

It has often been observed that after dense molecular clouds are formed, the physical conditions within them become more favorable for the production of complex molecular species in the gas phase relative to the conditions present in the diffuse ISM. Additionally, due to the low temperatures present within dense molecular clouds (~ 20 K), any polyatomic molecules bombarding the dust grains inside them tend to condense on the grain surfaces [39]. The accretion of simple polyatomic molecules on the ISD grain surface can lead to the formation of an icy mantle. This condensed mantle of accreted molecules is a chemically active region that can support numerous ionic and radical reaction processes within it. A large portion of this complex solid-state chemistry is driven by cosmic radiation, stellar shock waves, thermal stimulation, and UV photons (Fig. 4). Hydrogen also tends to play a key role in enhancing the molecular diversity present on grain surfaces [40]. This overall enhanced degree of reactivity within the mantle could be responsible for the observed abundance of simple interstellar polyatomic molecules in the condensed phase as compared to their gas phase counterparts within these cloud regions (Table 4).

As the most abundant element within the icy mantle (followed by carbon, nitrogen, and oxygen), hydrogen regulates gas-grain chemistry in a manner based upon the H/H_2 ratios present in the gas. Regions with greater H/H_2 ratios yield hydrogenated/reduced species like NH_3 , CH_4 , and H_2O , forming a hydrogen-rich polar mantle. Regions with lower H/H_2 ratio yield species like N_2 , O_2 , CO_2 , and CO , subsequently forming a more hydrogen-deficient, oxidized non-polar mantle [48].

During the gradual warm up in regions of massive star formation known as hot cores, where temperatures can rise to 200 K, the more strongly bound heavy radicals can become mobile on grain surfaces: this is thought to be the most crucial step for the formation of complex organic molecules within the mantle [49]. Ice evaporation in these hot, dense regions enriches the gas phase abundances of molecules, and the formation of many hot-core molecules has been attributed to this [50]. It is assumed that thermo-chemical processes occurring within the ice layers accreted on inorganic dust particles may also form a macromolecular organic residue that contains amino acid precursor structures.

3.3 *Radiation Dosage on the Icy Grain Mantle Surface*

Interstellar grains are produced and evolve under continual exposure to cosmic radiation. The radiation dosage to which the surface of ISD grains is exposed depends upon surrounding interstellar environments. The ISD grains found within the interiors of dense clouds are protected from intense galactic cosmic radiation by the outer cloud structure but are exposed to more deeply penetrating UV/IR

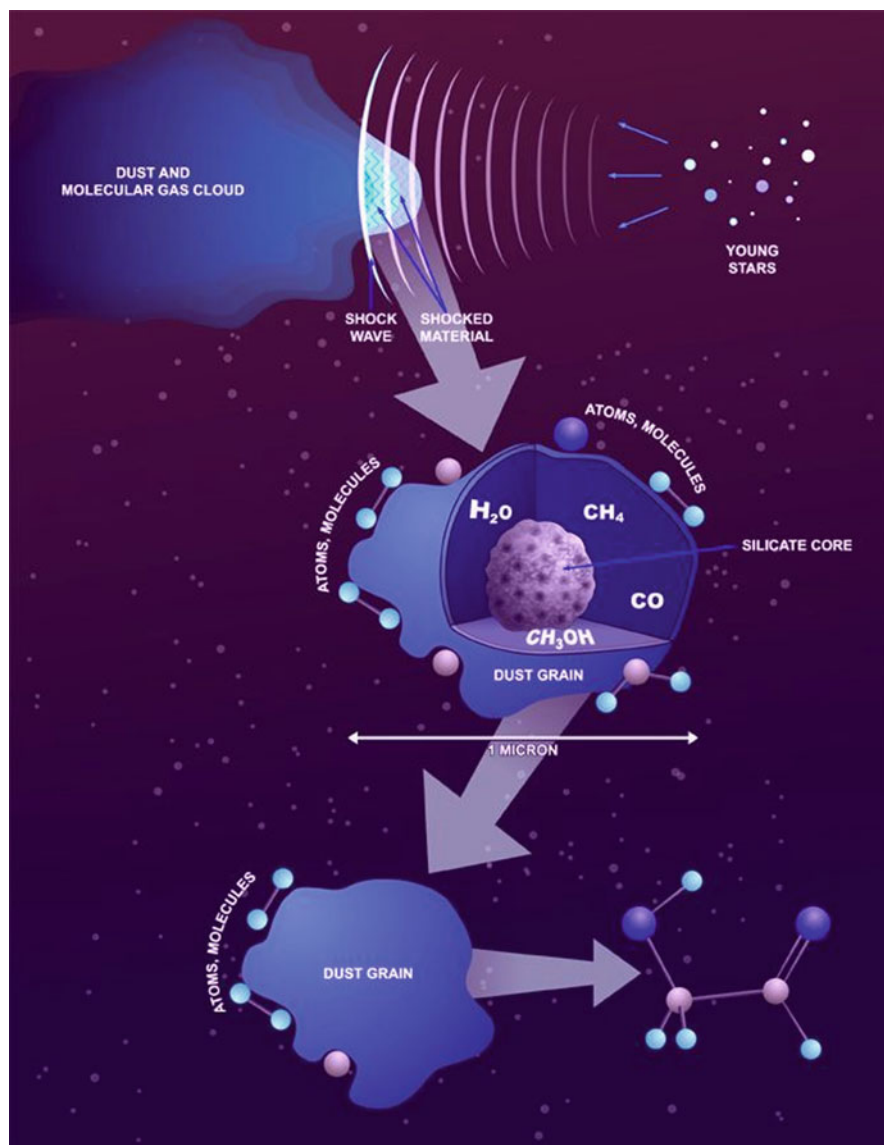


Fig. 4 Artistic impression of the synthesis of complex organic molecules on an interstellar dust grain surface. Young stars emit radiation and shock waves to liberate matter from molecular clouds. These molecular clouds are usually composed of dust and simple polyatomic molecules. At very low temperatures, simple molecules tend to accrete on the grain surface and develop into an icy mantle. The development of an icy mantle occurs at the same time that the IDPs are exposed to the radiation and stellar shock waves that ultimately assist in the interstellar synthesis of complex organic molecules (image credits: Bill Saxton, NRAO/AUI/NSF)

Table 4 Comparison between condensed and gas phase abundances of polyatomic molecules^{a,b,c}

Molecule	Condensed phase				Gas phase		
	TMC-1 ^{a,d}	OMC-1 ^{a,e}	ρ Oph-A ^{a,f}	NGC 7538 IR9 ^b	TMC-1 ^c	OMC-1 ^a	ρ Oph-A ^a
CH ₄	—	—	—	6×10^{-7}	—	—	—
CO ₂	37	10	22	8×10^{-6}	5×10^{-8}	$3\text{--}7 \times 10^{-7}$	$<6 \times 10^{-8}$
CO	19	0	5.6	6×10^{-6}	8×10^{-5}	1×10^{-4}	5×10^{-5} ^c
CH ₃ OH	—	—	—	6×10^{-6}	2×10^{-9}	1×10^{-7}	—
H ₂ O	100	100	100	6×10^{-5}	$<7 \times 10^{-8}$	$1\text{--}8 \times 10^{-8}$	3×10^{-9}
NH ₃	—	—	—	6×10^{-6}	2×10^{-8}	—	—

^aCondensed phase abundances are relative to water being 100%; gas phase abundances are relative to hydrogen [41]

^bCondensed phase mantle abundances [42]; CH₄ [43]; CO₂ [44] (units: molecules cm⁻²)

^cGas phase abundances: TMC-1 [45]; H₂O [46]; OMC-1 [47] (units: molecules cm⁻²)

^dCondensed phase mantles are not observed in TMC-1. They are approximated from the Taurus source Elias 18 that has an approximately same declination and ascension [46]

^eData measured from the ISO spectra for the source Orion IRC2 [41]

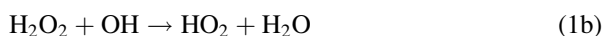
^fData obtained for the line of sight to Elias 29, a protostar with low mass [43]

radiation. Here, larger and more complex organic molecules can occur within the bulk material of the mantle and/or larger clusters [51].

Grains present in the exterior of dense clouds or in diffuse interstellar regions can experience heavy doses of cosmic and X-ray radiation and solar winds: this exposure can actually result in disruption of the structural integrity of the grain itself. Numerous interstellar simulation experiments have been conducted to study the effect of various wavelengths and types of radiation on the chemical evolution of icy grain mantles. The chemical effects of radiation exposure on a parent set of molecules and the subsequent synthesis of new molecular species have been studied extensively over the past two decades. The parent set of molecules in these simulations remains well-defined (CO, CO₂, NH₃, CH₃OH, and H₂O), as the effects of defined radiation doses on organic substrates during interstellar simulation experiments have proven difficult to analyze. Thus the effects of particular radiations onto a well-defined interstellar ice analogue, with defined frequencies and wavelengths, have been the foci of most previous studies. However in the real world the icy mantle experiences radiation of varying intensities often simultaneously.

In regions of high atomic hydrogen abundance, the most dominant species present within the icy mantles of interstellar dust particles (IDPs) has been observed to be condensed water. Water ice is known to exist in up to 17 different phases within the icy mantles, and these phases can be amorphous and/or crystalline in nature. Crystalline water ice is usually formed at temperatures above 130 K and hence is not abundantly present on interstellar icy grain mantles [52]. One experiment studying the effect of soft X-ray radiation on water ice has been reported by a research team from Laboratoire de Chimie-Physique, Université Pierre et Marie Curie and Laboratoire des Collisions Atomiques et Moléculaires, Université Paris Sud 11 in France. A porous amorphous solid water film composed of ultrapure

water and of a thickness of 120 monolayers was prepared by isotropically doping from a background pressure of 1.2×10^{-4} Torr, and considering the sticking co-efficient of water as unity. This film was grown on a clean Pt(1 1 1) single crystal and was then mounted on a rotatable sample holder maintained at 20 K in a thermally-controlled helium cryostat. Films were irradiated with a monochromatic X-ray radiation and with an unmonochromatized white beam at the synchrotron Lure SuperACO, Orsay on the bending magnet beamline SA22. Using near-edge X-ray fine absorption spectroscopy (NEXAFS) measurements, the team observed irradiation radical and molecular species such as OH, O₂, O, HO₂, and H₂O₂ [53]. However, H₂ and H were not detected. The species HO₂, H₂O₂, and O₂ were likely evolved during the annealing process occurring between 20 and 50 K, and their formation was possibly catalyzed by the presence of OH radical:



A similar experiment was conducted with another abundant interstellar molecule, CO. This CO ice simulation sample was prepared within a novel ultra-high vacuum interstellar astrochemistry chamber (ISAC) at the Centro de Astrobiología, Madrid [54]. The CO ice used was of 99% purity and was deposited on a CsI window maintained at 8 K on a cold-finger within a closed-cycled He-cryostat. Numerous irradiations investigating the effects of different ice layer thicknesses and irradiation times were conducted. The observed irradiation products of these CO ices were CO₂, C₂O, C₃O₂, C₃, C₄O, and CO₃/C₅ [55]. The possible evolution of these molecules can be represented in the following reactions:



The soft X-ray irradiation of CO and H₂O in ice grain simulation experiments provides insight into the possible ionization products that could be present on the mantle surface as well as within its vicinity. Hard X-rays in interstellar space are

highly penetrative and can ionize the grain through to its core. Such complete ionization would make it very difficult to observe higher order molecules on grain surfaces in regions with highly ionizing radiation.

Water-dominated ices yield the first order product OH^{\cdot} and higher order products such as HO_2^{\cdot} and H_2O_2 upon exposure to UV radiation, a condition widely presumed to exist in dense media. However addition of CO to a water-dominated UV-irradiated system can also yield species like CO_2 , H_2CO , HCO , and HCOOH [55]. There is little evidence for the formation of any higher mass polymeric molecules in the ISM. The presence of ISD, rich in organic molecules itself, makes detection of fine spectroscopic signatures from interstellar space even more difficult. This is indeed one of the main reasons why it has been difficult to date to detect amino acids and similar molecules in interstellar space. This limiting factor of detecting more complex organics is a limitation inherent to astronomical spectroscopy and has led to the development of simplified laboratory interstellar simulation experiments to understand and recreate those physico-chemical processes that are currently largely undetectable by astronomical technology to date.

3.4 Accretion of Organics on Icy Mantles

An interstellar grain with an icy mantle is not a stable substrate. It is indeed chemically dynamic and there is much to consider in terms of the possible physico-chemical processes occurring within IDPs. The polarity attained by an icy mantle, which is dictated by H_2/H ratios, should allow separation of the grains within the mantle into polar mantle grains and non-polar mantle grains [56]. Even if layer thickness is standardized, the time required for the development of each new layer can vary. Accretion of layers is considered to occur efficiently at the low temperatures extant in interstellar space (~ 15 K). This accretion of layers facilitates chemical reactivity within IDPs, with layer accretion occurring on a timescale of $\sim 2 \times 10^9/n(\text{H}_2)$ yr, if the sticking efficiency is assumed as unity [56]. If the simplified scenario of accretion within generic dense cloud media is considered, the formation of ices on IDPs can be considered to result from either of two separation mechanisms: diverse condensation (DC) and diverse desorption (DD) [57].

The DC model proposes that the polar and non-polar components of interstellar ice mantles are affiliated with dense regions of varying visual extinction and densities. The model asserts that condensation at densities $2 \times 10^3 \text{ cm}^{-3} < n_{\text{H}} < 2 \times 10^4 \text{ cm}^{-3}$ yields water-dominated ice mantles with diverse volatile inclusions of species such as CO, CO_2 , O_2 , N_2 , and CH_3OH . Each of these inclusions are condensed at their respective condensation densities; for example, mantles with CO, O_2 , and N_2 are obtained at condensation densities $n_{\text{H}} > \sim 10^5 \text{ cm}^{-3}$ [57].

Within the DD model, the differential composition of H_2O -dominated ices and non-polar ices indicate a difference in their volatility. This model states that initial condensation produces homogenous ice with abundant volatile inclusions like those

mentioned above. Selective desorption would deplete volatile inclusions from within the mantle and allow these volatiles to recondense on top of the original ice. Thus in the DD model the H₂O-dominated ice is the “original” ice and the recondensed volatile inclusions are considered to be the “non-polar” ice. This model predicts the formation of recondensed non-polar ice mantles of diverse molecular and elemental composition [57].

4 The Formation of Amino Acids and the Origin of Homochirality in Interstellar Space

The search for the origin of the universe’s biomolecules continues to capture the human imagination. However, there are many physicochemical conditions that would have had to be necessary in order for amino acid synthesis to have originally occurred in interstellar space. Some of these necessary conditions would likely have included a dusty environment, appropriate radiation dosage, appropriate stoichiometry of molecules, and appropriate sources for molecular asymmetry.

4.1 *Asymmetry Propagates Asymmetry*

Asymmetry is observed in all of the biomolecular molecules that constitute life: proteins, carbohydrates, RNA, and DNA. For the purposes of biological organics, a molecule is asymmetric if at least one carbon atom within the molecular structure, called the stereogenic center, has four different atoms or groups attached to it. If a molecule is asymmetric, or chiral, this necessarily also implies that it has a mirror image, known as an “enantiomer.” If one enantiomer is present in larger quantities in a given environment than the other enantiomer, an enantiomeric excess (ee), or asymmetrical bias, occurs. However, in order for a molecule to be enantioenriched, it must have been synthesized in an asymmetric environment (Fig. 5).

There currently exist two main accepted models for the creation of asymmetry in our universe: (1) parity-violation by the weak nuclear force; and (2) the presence of chiral fields such as circularly polarized light (CPL).

The parity-violating weak force, mediated by the Z⁰ boson, can influence molecules either (1) by altering the energies and energy levels imparting a parity violating energy difference (PVED) between enantiomers [58] or (2) by the interaction of spin-polarized electrons with matter following β -decay. In 1966, Yamagata reported that there exists a small difference in energy between enantiomers due to parity violation and addressed possible consequences both for molecular chirality and biomolecular homochirality [59]. Consideration of the parity-violating weak interaction indicates that L-amino acids are stabilized with respect to D-amino acids [60–62]. However, recent quantum-chemical ab initio

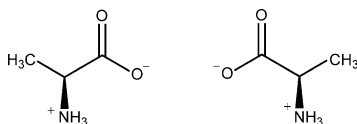


Fig. 5 The zwitterionic enantiomers of the amino acid alanine: L-alanine (*left*) and D-alanine (*right*). Alanine is the simplest chiral amino acid

calculations, particularly those of Quack and co-workers [63] and Schwerdtfeger et al. [64], have shown that the magnitude and indeed the sign of the PVED depend upon the exact molecular conformation of the species being considered. Moreover, parity violation leads to energy differences between enantiomers in the femtojoule to picojoule per mole range – this makes experimental observation of these differences difficult to perform. The small values of PVED for biological molecules composed only of light atoms have prompted chemists to doubt that the parity violating term could give rise to the distinct chirality of molecules observed in living nature.

The use of spin-polarized electrons as a source of chiral asymmetry has scarcely been employed in chemical reactions, even though this radiation might also have played an important role in the origin of molecular chirality [65]. Spin-polarized electrons can be generated as a result of parity violation in nuclear β -decay products [66]. A chiral molecule will be ionized at different rates by longitudinally spin-polarized electrons, as proposed by Vester and Ulbricht in 1962 [67]. Upon passing through matter, spin-polarized electrons decelerate and this deceleration results in the emission of circularly polarized electromagnetic radiation. These “chiral photons” can then interact with racemic or prochiral organic molecules via asymmetric photoreactions in order to induce an enantiomeric excess. However, again due to laboratory limitations in the detection of the very small asymmetry inducible by the Vester-Ulbricht process [68], experimental verification of this phenomenon remains inconclusive.

Currently the most promising external physical agent to induce optical activity in molecules appears to be CPL. The potential use of either *right*-handed or *left*-handed CPL (*r*-CPL or *l*-CPL) to induce enantiomeric enrichment into originally racemic mixtures was recognized by the end of the nineteenth century by van’t Hoff and Le Bel. When a racemic mixture of molecules with sufficiently small and excited electronic state barriers to enantiomer inversion is irradiated with CPL at wavelengths of significant circular dichroism (CD), the initial equality of the enantiomers in the ground state will change. The concentration of the more strongly absorbing enantiomer will decrease, and that of the other will increase, resulting in a measurable enantiomeric excess (ee). From a mechanistic viewpoint, photochemical induction of optical activity with CPL can occur via different pathways: (1) absolute asymmetric photolysis (preferential decomposition of one enantiomer of a racemic mixture); (2) absolute asymmetric photosynthesis; or (3) photoisomerization between enantiomers [69–71]. A number of enantio-differentiating photoreactions initiated by CPL have already been successfully achieved [72–79]; thus the

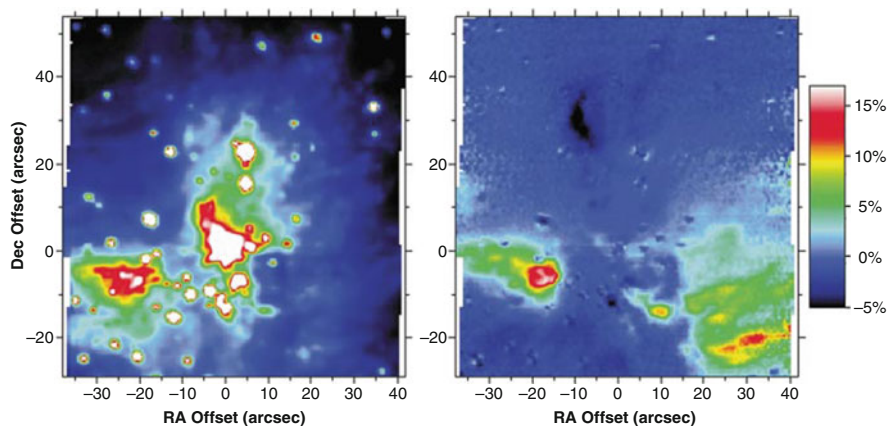


Fig. 6 Circular polarization (CP) map of the Orion Molecular Cloud-1 star formation region at $2.2\ \mu\text{m}$. *Left*: total infrared intensity of CP map of OMC-1. The typical size of the protostellar disk is much smaller than the observed structure of polarization. *Right*: percentage circular polarization at IR wavelength is observed to vary from 17% (dark region) to +5% (white region) [81]. Reproduced by permission of AAAS

observation of interstellar CPL and the role it could play in determining interstellar asymmetric molecules is therefore of great interest.

Although neutron stars were originally thought to be a source of CPL in interstellar space, this theory has since been discarded due to the fact that CPL has not been observed within the UV and visible wavelengths of light that they emit [80]. It is currently thought that star-formation regions, particularly those regions containing solar-mass stars and their planetary systems, were and continue to be the main source of CPL in the universe. This theory has been substantiated by the detection of CPL at IR wavelengths using the 3.9 mm Anglo-Australian Telescope along with a polarimetry system within the Orion Molecular Cloud Complex (OMC-1) [81]. The OMC-1 is a massive star-forming region at a distance of approximately 1,500 light years from Earth. Near IR circular polarization images of OMC-1 depict a quadrupolar distribution of left-handed and right-handed CPL, with the majority of light emission centered on a young luminous star known as IRC2 [82, 83]. The largest amount of CPL observed was from a region of a reflection nebula that scatters light from the Orion IRC2 region. The percentage of CPL observed in this region was as high as 17% at IR wavelengths (Fig. 6). These values of CPL detection are much larger than those previously observed from low mass stars emitting CP of around 1–2% [84]. Yet it is UV-CPL and not IR-CPL that is capable of inducing enantiomeric excesses in the molecules within the mantle being synthesized/degraded by it. It is thought that no UV-CPL has yet been detected from OMC-1 for this very reason: UV-CPL is readily absorbed by ISD and therefore does not make its way to astronomical detection systems [81].

Non-spherical ISD grains are, however, also thought to contribute to the CPL produced by star-forming regions via a process called dichroic scattering of linearly

polarized light (LPL). During this process, non-spherical dust grains become aligned to the direction of the LPL, and the axis of the dust's greatest rotational angular momentum rotates about the surrounding magnetic field to create a dichroic scattering phenomenon [85]. Whether these aligned dust grains produce CPL as well as produce asymmetric organic molecules within their icy mantles remains debatable.

The scientific community is now investigating the history of how and when our solar system might have been exposed to asymmetric CPL. Our sun is a low-mass star like those found in star-forming regions such as the OMC-1. The confirmed presence of ^{60}Fe in meteorites suggests the occurrence of a supernova explosion near our solar system and further implies that the solar system was formed in a huge star-forming region that would have continuously been emitting CPL. ^{60}Fe is a radioisotope with a half-life of 1.5 Myr and can provide a means for dating these explosions. Recently the rate of occurrence of supernovae explosions in the solar vicinity (<0.85 kpc) has been studied, and it would appear that the Earth was exposed to supernovae explosions around 372.6, 269.1, 140.6, and 17.3 Myr before the present day [86].

Although close proximity to supernovae would result in destruction of any ice grain chemistry, studies conducted by ESA's Integral Observatory have indicated that supernovae explosions occur every 50 years in the Milky Way galaxy and likely play a crucial role in catalyzing interstellar chemistry [87]. Supernovae are one of the main sources of ISD in the universe. It is thus possible that dust from remnant supernovae that had been strewn far away from its explosion source originally accreted polyatomic molecules within an icy mantle that was simultaneously irradiated by UV-CPL emitted from a moderately proximal star-forming region.

4.2 The Detection of Amino Acids in Interplanetary Space

Amino acids form an integral part of all structural and functional biomolecular processes occurring in all living organisms. However, the origin of amino acids and their role in the evolution of life remain questions unanswered within the scientific community, despite decades of investigation. It still remains uncertain whether amino acids were originally formed terrestrially or extra-terrestrially, and the origin of their homochirality is also currently unknown.

Amino acids can be readily formed from precursor molecules such as formic acid and acetic acid. These small volatile molecules are detected in abundance in the ISM even though amino acids remain undetected in interstellar space. However, the observation of glycine in the cometary samples collected by the Stardust space-probe [88] indicates that amino acids could potentially be found in interplanetary space. The discovery of nearly 90 monoamino and diamino acids in the Murchison meteorite that fell to Earth in 1969 in Murchison, Australia [89] suggests the possibility that amino acids formed extraterrestrially could have originally been

delivered to Earth by interstellar bodies. Meteorites are fragments of extraterrestrial matter – mostly propelled from asteroids into Earth-crossing orbits – that eventually fall to Earth's surface. The insoluble organic matter of the Murchison meteorite is significantly enriched in deuterium and ^{15}N [90]. Similar bulk isotopic enrichments have been found in chondritic IDPs and comet Wild 2 samples, suggesting that there is an evolutionary link between organics in meteorites and comets. Analyses of Murchison meteorite samples have been found to contain several natural and non-natural amino acids among the carbonaceous fragments, with a slight preponderance of L-enantiomers relative to D-enantiomers [91–94]. Interestingly, there was an even higher occurrence (up to 18.5%) of the L-form of several α -methyl substituted amino acids such as isovaline and α -methylnorleucine [94]. The fact that only L-amino acid excesses have been found in carbonaceous meteorites analyzed so far may indicate an extraterrestrial origin for life on Earth and that this life was biased toward L-amino acid homochirality from the very beginning.

5 Production of Amino Acids in Laboratory Simulation Experiments

Numerous laboratory interstellar ice mantle simulation experiments dedicated to the synthesis of amino acids have been conducted in hope of furthering understanding how amino acids might have been synthesized in the ISM. The experimental set-ups commonly used for these investigations involve standardized low pressures (10^{-7} mbar) and low temperatures (10–100 K) to simulate realistic interstellar conditions. The condensed gas mixtures used are chosen to be representative of ices formed near protostellar sources and are mostly deposited on a metal or inert metal-salt window mounted on an icy finger to form a condensed film of pre-specified dimensions. During the experiment, the condensed gas mixture is irradiated with UV light of particular wavelengths. After irradiation exposure, the sample is warmed slowly to room temperature and is derivatized and analyzed using different analytical techniques – the most common of these are GC–MS, GC \times GC–MS, HPLC, and IR spectroscopy. Contamination of samples can be excluded with the use of isotopic labeling [95].

5.1 *Laboratory Studies on Amino Acid Formation in Interstellar Ice Analogues*

Two independent simulation experiments were conducted by Bernstein et al. [96] and Muñoz Caro et al. [95] in 2002 where they irradiated their respective samples with non-polarized UV light. Bernstein et al. [96] used an ice mixture containing $\text{H}_2\text{O}:\text{NH}_3:\text{CH}_3\text{OH}:\text{CH}_3\text{CN} = 20:2:1:1$ (molar composition); the ice mixture after

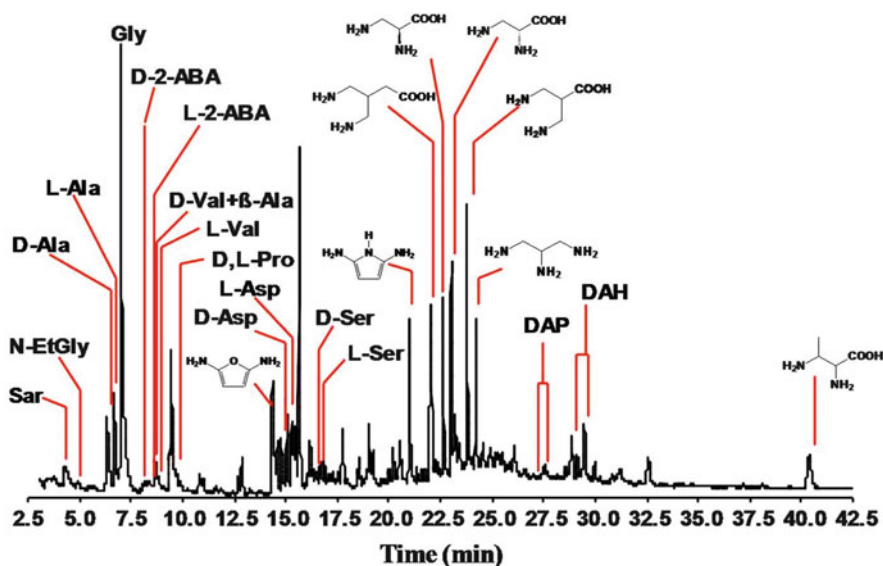


Fig. 7 Gas chromatogram of an ice mixture $\text{H}_2\text{O}:\text{NH}_3:\text{CH}_3\text{OH}:\text{CH}_3\text{CN} = 2:1:1:1$ (molar composition) prepared under realistic circumstellar/interstellar conditions by Munoz Caro et al. [95]. The ice mixture was irradiated, warmed to room temperature, hydrolyzed with acid, and derivatized. Sixteen product amino acids were observed as racemates using enantioselective gas chromatography mass spectrometry (GC–MS). Two diamino acids were also detected: DAP (diaminopentanoic acid) and DAH (diaminohexanoic acid)

irradiation was warmed to room temperature and compositionally analyzed using GC–MS and HPLC. The amino acids serine, glycine, and alanine were detected as products from this interstellar ice simulation.

Munoz Caro et al. [95] used another ice mixture that specifically avoided preformed carbon-nitrogen bonds in the precursor gas molecules. This condensed gas mixture contained $\text{H}_2\text{O}:\text{}^{13}\text{CH}_3\text{OH}:\text{NH}_3:\text{}^{13}\text{CO}:\text{}^{13}\text{CO}_2 = 2:1:1:1:1$ (molar composition). CO is a dominant interstellar molecule relative to acetonitrile and both CO and CO_2 are thought to play a crucial role in enhancing the diversity of amino acid production. In order to exclude any terrestrial contamination, isotopic ^{13}C -labeled reactants were used in this interstellar ice simulation experiment. After irradiation, the sample was allowed to warm to room temperature, hydrolyzed, derivatized using ECEE, and further analyzed by enantioselective GC–MS. From this simulation, 16 amino acids out of which 6 were proteinogenic amino acids were detected. Although the numbers of amino acids formed in both these experiments differ, one common result in both simulations was the high amount of glycine detected (Fig. 7). Thus both of these investigations would appear to indicate that glycine should be abundantly formed in ISM [97, 98].

Both teams further indicated that the identified amino acids are likely originally parts of peptidic or oligomeric structures that form within the organic residue of interstellar ice analogues and are released as free molecules after additional acid

hydrolysis. The UV-photoprocessed interstellar residue may form exothermically from recombined radicals which are able to diffuse and react within complex radical chain reactions in the slow melting ice [99]. The precise reaction pathways and channels, however, are not yet fully understood (see Sect. 5.4).

A more recent experiment by Meinert et al. [100] has involved the exposure of an interstellar ice analogue containing $\text{H}_2\text{O}:\text{}^{13}\text{CH}_3\text{OH}:\text{NH}_3 = 2:1:1$ (molar composition) to UV light at 121 nm. The mixture was deposited on MgF_2 window and simultaneously irradiated for a period of 10 days. After irradiation the sample was extracted in H_2O , hydrolyzed using 6 M HCl, derivatized, and analyzed using enantioselective two-dimensional gas chromatography coupled to time-of-flight mass spectrometry (GC \times GC-TOFMS). A total of 20 amino acids and 6 diamino acids have been identified in the organic residue, including proteinogenic amino acids such as serine, proline, aspartic acid, alanine, glycine, and the diamino acid *N*-(2-aminoethyl) glycine.

5.2 Asymmetric Photochemistry and Anisotropy Spectra of Amino Acids

Given that amino acids are abundantly present in living organisms in predominantly one enantiomeric form, the simulated synthesis of amino acids in interstellar environments must inevitably incorporate the induction of asymmetry. Thus, the next step in designing interstellar ice simulation experiments of amino acids was to consider the effect of CPL on both the synthetic and photolytic chemistry that might be occurring in the ice mantle of IDPs. The first of these investigations exploring photosynthesis was performed at the DESIRS beamline of the SOLEIL synchrotron facility in France [101, 102]. A condensed gas mixture was irradiated with UV-CPL radiation under simulated interstellar conditions. The condensed gas mixture used consisted of $\text{H}_2\text{O}:\text{}^{13}\text{CH}_3\text{OH}:\text{NH}_3 = 2:1:1$; the methanol carbon was isotopically labeled in order to ensure that any contamination that might have occurred during the experiment could be accounted for during analysis. The condensed gas mixture was irradiated with VUV-CPL of either right helicity (*r*-CPL) or left helicity (*l*-CPL) at low temperature ($T = 80$ K) for 36 h. The sample was then warmed slowly to room temperature and analyzed using GC \times GC-TOFMS. Enantiomeric excesses of either L-alanine or D-alanine (up to 1.34% ee) were observed, depending on the handedness of the CPL, and these enantiomeric excesses were found to be proportional to the number of photons absorbed per ice molecule. Encouragingly, the enantiomeric excesses detected approximate those observed for alanine detected previously in meteoritic sample extracts (1.2% ee).

This research, however, does not address the mechanism for amino acids synthesis in extraterrestrial environments and how they continued to exist while associated with larger interstellar bodies prior to their descent to Earth. It is thought that upon formation on their parent bodies, amino acids might have agglomerated

into polymeric states that would have rendered them invisible to astronomical spectroscopic detection [103]. The circumstantial evidence of the detection of monoamino and diamino acids in meteorite samples [104] and the ability of amino acids to form peptides and extended polymeric structures might support this theory; however amino acids in interstellar space, either in monomeric or polymeric form, remain undetected.

In order to understand the asymmetric photochemistry of amino acids and how UV-CPL might have facilitated the transfer of asymmetry from chiral massless photons to organic molecules, it has been necessary to attempt to characterize the interaction between CPL and amino acids. Enantiomers of a given amino acid absorb CPL differentially. This differential absorption (ΔA) is a function of CPL wavelength and can be expressed as CD. The CD spectra of a series of prebiotic amino acids have now been recorded in order to begin to characterize this interaction. Measurements of CD spectra ranging from 130 to 330 nm have demonstrated that the highest degree of effect of CPL on amino acids occurs in the vacuum UV (VUV) range between 130 and 190 nm where intense CD bands have been observed [105, 106] and calculated [107]. This VUV spectral range is not accessible if aqueous solutions of the amino acids are analyzed because water absorbs UV light below 200 nm. Therefore, in order to extend the range of CD measurements obtained, solid amorphous amino acid films were analyzed instead. The use of these films, of a pre-specified thickness, more accurately models the solid state in which amino acids would likely exist in interstellar environments.

More recently, an additional means of characterization of the interaction of CPL with chiral small molecules such as amino acids has been reported. In 2012 Meinert et al. [100] reported a series of characterizing anisotropy spectra of amino acids, stating that it is not exclusively the CD signal that influences chirality transfer from photons to amino acids. The anisotropy factor g , the ratio between CD signal and absorption, can be used to describe more accurately the behavior of the interaction between a chiral small molecule and CPL. Anisotropy factors of amino acids were previously only known for a few specific wavelengths. Anisotropy spectra have now been recorded for various isotropic amorphous amino acid enantiomers such as alanine and valine (Fig. 8) in the UV and VUV spectral regions: anisotropy factor g is described as a function of CPL wavelength. Use of anisotropy spectra to characterize the CPL-chiral molecule interaction will allow for prediction of reaction rates and the extent of ee achievable when conducting photochemical reactions of amino acids using CPL. Given that anisotropy spectra can be used to characterize asymmetric photochemical behavior, these data will certainly be used to investigate other families of chiral small molecules.

Using the data obtained from both CD and anisotropy spectroscopy of amino acids, a series of experiments has been performed investigating the photolysis mechanism for the generation of asymmetry in amino acids. Thin amorphous films of racemic amino acids in their solid state (e.g., alanine and leucine) have been subjected to CPL of given handedness and predetermined wavelengths. The irradiation wavelengths were chosen on the basis of the maxima and minima for ee generation as determined from CD and anisotropy spectra. Enantiomeric

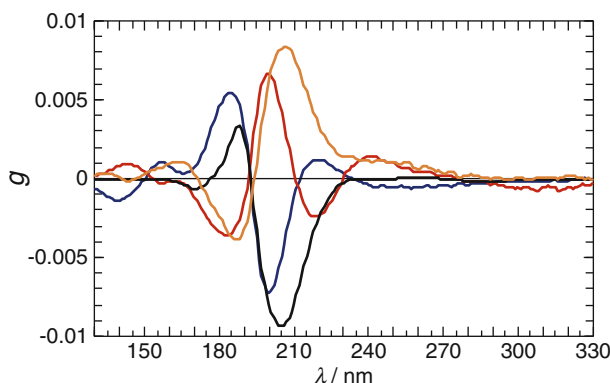


Fig. 8 Anisotropy spectra in the vacuum UV and UV spectral region of isotropic amorphous D-alanine (red), L-alanine (blue), D-valine (orange), and L-valine (black) enantiomers

enrichments of up to 5.2% ee have now been reported for the enantioselective photolysis of leucine by CPL [108–110]. The results of these systematic photochemical studies demonstrate that asymmetric photochemistry does have the potential to induce enantiomeric excesses of up to a few percent into amino acids in environments of high vacuum and low temperature.

5.3 Asymmetric Amplification Processes

To date, only small excesses of asymmetry in proteinaceous amino acids have been observed during analyses of both cometary ice simulation experiments and chondritic meteorite samples. How could these small excesses have evolved into the overwhelming enantiomeric preference for L-amino acids in all of today's living organisms? Several authors have addressed ways in which a small enantiomeric bias can be amplified. The Frank autocatalytic kinetic model for asymmetric synthesis suggests that even a slight excess of one enantiomer will influence and favor the synthesis of that enantiomer over the other. Over time, such a slight excess would thereby evolve into a dominant preference for one enantiomer over its opposite in a given system [111]. Kondepudi, et al. [112, 113] have demonstrated this concept within a number of autocatalytic systems to demonstrate its effectiveness (Fig. 9). Morowitz proposed that this model could be applied to the evolution of asymmetry in prebiotic amino acids in 1969, given the fact that most racemates of amino acids are less soluble than the crystals of either the D-enantiomers or the L-enantiomers. The reductive Zn-mediated alkylation reported by Soai, et al. in 1995 was the first truly autocatalytic asymmetric amplification, with greater than 99.5% ee observed [114]. Both Breslow and Blackmond have reported successful enantiomeric enhancement of amino acids by differential crystallization processes and autocatalytic asymmetry amplification [115–118]. Further research is certainly

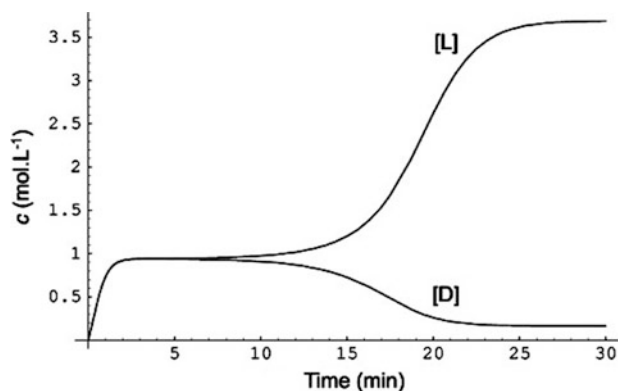


Fig. 9 Concept of autocatalytic amplification – autocatalytic amplification of the L-enantiomer (*upper branch*) over the D-enantiomer (*lower branch*) in the Kondepudi–Prigogine reaction sequence [112, 113]. A tiny ee of the L-enantiomer at $t = 0$ is increased to a high ee after only 30 min of reaction time

required in this field of asymmetric autocatalysis in order to provide a logical explanation of the evolution from achiral condensed gaseous mixtures to the asymmetric amino acids used in all biological processes today.

5.4 The Higher Order Structures of Amino Acids

In 2004 both monoamino and diamino acids were discovered in the CM type Murchison meteorite [104]. CM type carbonaceous chondritic meteorites have very high carbon content relative to other types of meteorites; hence these meteorites can provide a significant amount of information about what kinds of organic molecules might have been synthesized extraterrestrially and how these compounds might have been delivered to Earth. The meteorite analysis that afforded the detection of diamino acids in 2004 involved the extraction of a fresh sample of the Murchison meteorite using hot water hydrolysis and further analysis using an enantioselective chromatographic column on a GC–MS instrument. Efficient derivatization of the sample with ECEE resulted in the identification of six diamino acids of the type diaminoalkanoic acids. This finding correlated well with the identification of similar diamino acids (diaminopentanoic acid and diaminohexanoic acid) from the UV-irradiated interstellar ices simulations using a condensed gas mixture of $\text{H}_2\text{O}:\text{}^{13}\text{CH}_3\text{OH}:\text{NH}_3:\text{CO}:\text{CO}_2 = 2:1:1:1:1$ [95]. Recently, six diamino acids including the two enantiomers of D,L-2,4-diaminobutyric acid and, for the first time, the achiral *N*-(2-aminoethyl)glycine were detected after a similar interstellar ice experiment using enantioselective GC \times GC–TOFMS analysis (Fig. 10) [100]. These diamino acids are of particular interest given that they can participate in the formation of peptide nucleic acid

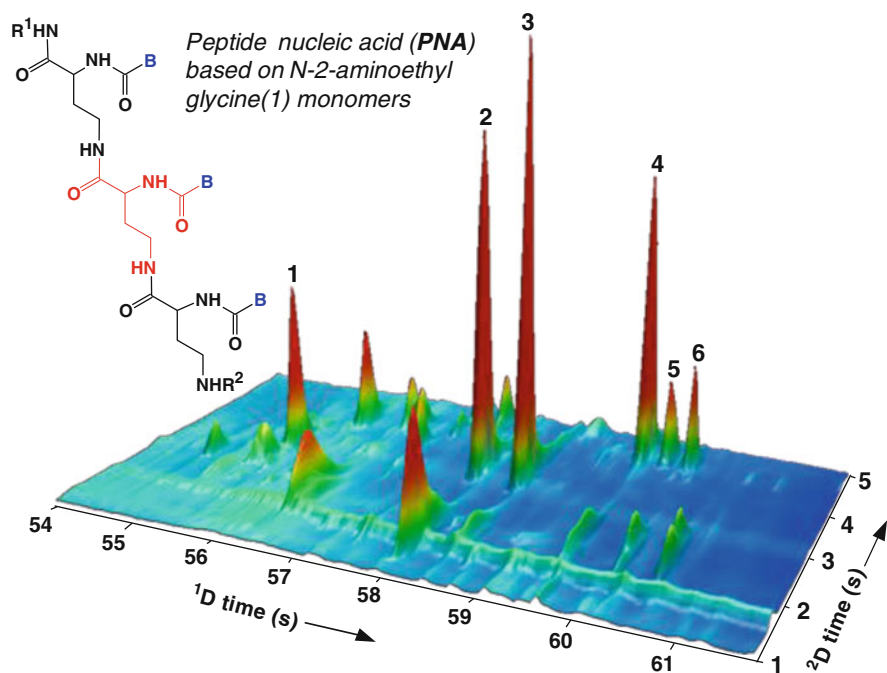


Fig. 10 Close-up view of the two-dimensional enantioselective gas chromatogram depicting derivatives of ^{13}C -labelled diamino acids (1) *N*-(2-aminoethyl) glycine, (2) *L*-2,3-diaminopropanoic acid (DAP), (3) *D*-2,3-DAP, (4) 3-amino-2-(aminoethyl) propionic acid, (5) *L*-2,4-diaminobutyric acid (DAB), and (6) *D*-2,4-DAB generated under simulated interstellar pre-cometary conditions [100]

(PNA) which might have served as the primordial genetic material [119]. PNA has been proposed to be a possible pre-RNA structure, whereby the sugar-phosphate molecular backbone of RNA and DNA evolved from an uncharged peptide backbone. [119]. This peptide-based backbone could have either been composed of *N*-(2-aminoethyl)glycine (aeg) (leading to aegPNA molecules) or of 2,4-diaminobutyric acid (da) (leading to daPNA structures). PNA can form stable double helices with complementary molecules of RNA or DNA, and this stability might indicate that PNA could have served as an initial evolutionary template.

The observation of amino acids, diamino acids, and other organic molecules [120–122] in interstellar ice analogues and in meteoritic samples indicates that there exist mechanisms via which exogenous organic molecules could have been delivered to Earth (Fig. 11). It is difficult to relate icy bodies and meteorites; both may carry amino acids formed by different mechanisms, or perhaps the meteorites analyzed to date that contain amino acids could have been remnants of an icy comet. Thus the next step in understanding the origin and evolution of amino acids in extraterrestrial environments is to attempt the search for amino acids on actual interstellar bodies. The COSAC instrument on the ESA mission ROSETTA is

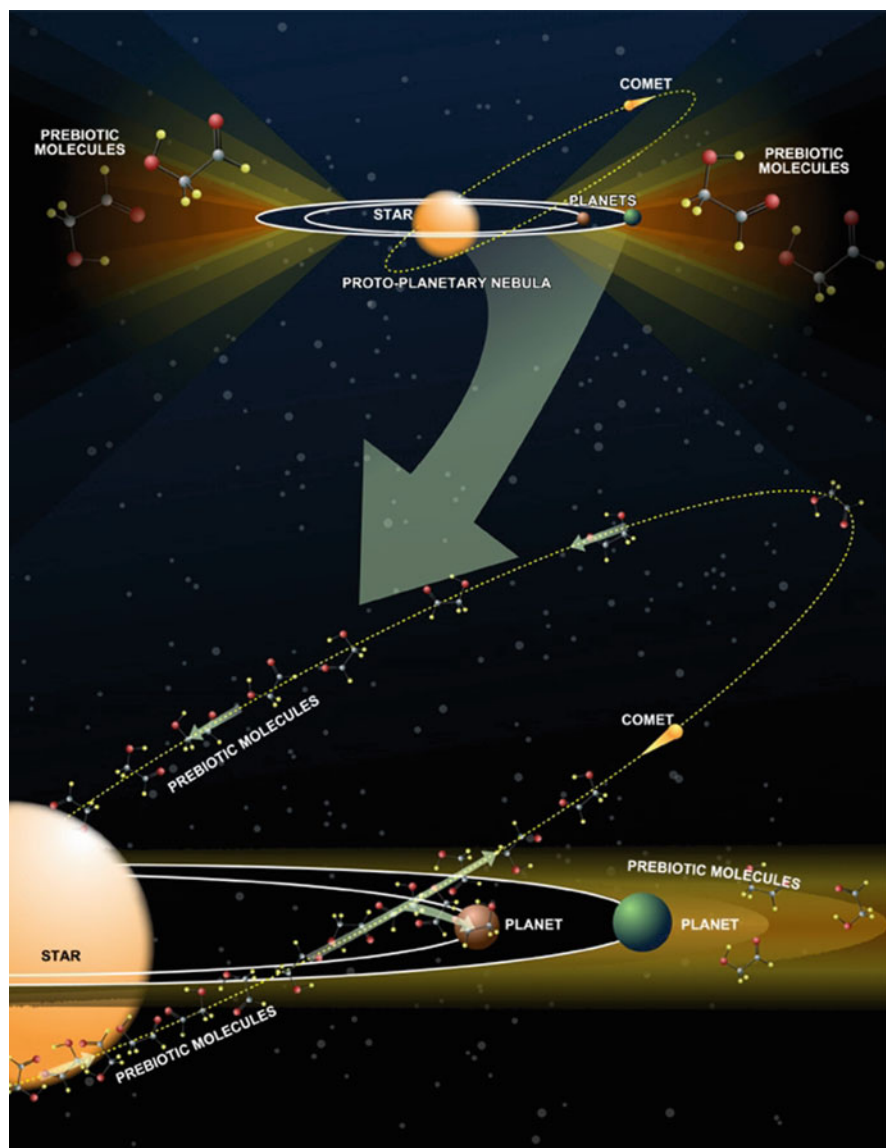


Fig. 11 Artistic impression of the possible journey of prebiotic molecules from comets to planets. Comets and meteorites are important delivery agents of interstellar organic molecules to Earth and other planets (image credits: Bill Saxton, NRAO/AUI/NSF)

intended to achieve this goal and conduct thorough chemical analyses on the surface of the comet 67P/Churyumov-Gerasimenko in order to determine the existence of interstellar amino acids and other chiral organics.

6 The COSAC Experiment on ROSETTA: The First Advances

In the mid-twentieth century astronomers began studying comets using ground based telescopes, analyzing multiple electromagnetic spectral regions. However remote observations cannot always afford certain desired answers. Thus with advances in space exploration the European Space Agency (ESA) envisioned an in situ exploration of a cometary nucleus.

In the late 1970s the ESA proposed a close fly-by of the comet 1P/Halley (Halley's comet), due to approach its perihelion in 1986 [123, 124]. This fly-by mission was called GIOTTO after the famous Italian renaissance painter Giotto di Bondone. GIOTTO was launched on an Ariane 1 rocket on 22 July 1985. It successfully flew past 1P/Halley on 14 March 1986 and was later commanded to fly past another comet, 26P/Grigg-Skjellerup, on 10 July 1992 [125]. This significant mission was the first to afford close analysis of the shape and size of both of these two comets, providing accurate dimensions and compositional and velocity estimates of the dust particles and the gases emitted. The GIOTTO mission was considered a technological landmark and changed the perception of comets as proposed by the earlier cometary sandbank model. It actually confirmed that comets do possess a solid and cohesive structure and lent hope to the prospect of landing on a cometary nucleus [126]. This cometary nuclear landing is the envisioned goal of the first ESA cometary surface exploration mission ROSETTA.

ROSETTA was approved in the year 1993 as a Planetary Cornerstone Mission of ESA in its Horizon 2000 long-term program. A successor to GIOTTO, ROSETTA's principal objective is to study the origin of comets and to understand the origin of the solar system by attempting a landing on Comet 67P/Churyumov-Gerasimenko [125, 126]. The ROSETTA mission physically consists of two mission elements – the lander PHILAE and the orbiter ROSETTA. The mission was originally designed to study the comet 46P/Wirtanen but a launch failure of an ESA rocket Ariane 5 in December 2002 led to a postponement of the mission and a new target comet was required. The comet 67P/Churyumov-Gerasimenko was identified and the mission was redesigned for this new target. ROSETTA was finally launched on 2 March 2004 by an Ariane G + rocket from the Guyana Space Center in Kourou, French Guyana [127]. ROSETTA's journey includes four planetary gravity assist maneuvers in the sequence Earth–Mars–Earth–Earth in order to acquire sufficient thrust to reach 67P. It is planned to reach comet 67P in November 2014 after 10 years of flight time through the Solar System.

6.1 PHILAE Lander and COSAC

The PHILAE Lander is an ambitious indigenous element of the ROSETTA mission that will be detached from the orbiter to land on the cometary nucleus (Fig. 12). The Lander, previously known as ROLAND, was proposed by a team of scientists led



Fig. 12 Artistic impression of Philae Lander on the surface of comet 67P/Churyumov-Gerasimenko. Philae is planned to soft land on the cometary nucleus in November 2014. The landing site will be determined by the Rosetta team after a close approach to the comet (image credit: ESA)

by Dr. Helmut Rosenbauer from the Max Planck Institute for Solar System Research in Katlenburg Lindau, Germany. The Lander system has integrated within it ten scientific instruments and sub-systems provided by various space agencies and research laboratories from six European nations; its landing and the analytical study of the cometary surface is overseen by ESA. A complete description of the PHILAE Lander system can be found in “The ROSETTA Lander (‘PHILAE’) Investigations” [128]. Apart from a wide range of instruments targeted to study the various aspects of the comet 67P, the cumulative activity of sample drilling and acquisition is of particular importance to analyze the composition of the cometary nucleus. The drilling and sample acquisition activity has been assigned to the Sampler, Drill, and Distribution (SD-2) system. Analysis of the acquired surface sample will be performed by (1) the cometary sampling and composition (COSAC) experiment to investigate the molecular and stereoselective composition; (2) PTOLEMY for isotopic measurements composition; and (3) the comet infrared and visible analyzer (CIVA) for infrared imaging and microscopic measurement of the sample (Table 5). The sample collected by SD-2 will be first measured by CIVA prior to delivery to PTOLEMY and COSAC [129].

The COSAC Experiment consists of an instrumental suite of a gas chromatograph (GC), a time-of-flight mass spectrometer (TOFMS), and an allied electronic system allowing remote operation of the suite (Fig. 13). The GC–TOFMS instrument performs the separation, identification and quantification of the individual components from a mixture of volatile molecules.

The COSAC Experiment is designed to meet payload specifications since there are strict limitations of size, power, mass, and resources involved in a space mission. The GC detectors, valves, and carrier tanks have been miniaturized to

Table 5 The sample acquisition and analysis instrumental suite onboard PHILAE

Instrument	Purpose	Contributing organization
SD-2	Sample drilling and acquisition	Politecnico di Milano, Milan, Italy
COSAC	Molecular and chirality analysis of sample	Max-Planck-Institut für Sonnensystemforschung, Katlenburg-Lindau, Germany
PTOLEMY	Isotopic analysis of sample	Planetary and Space Science Research Institute, The Open University, Milton Keynes, England
CIVA	Optical imaging, infrared spectral imaging and microscopic analysis	IAS, Institut d'Astrophysique Spatiale, Orsay, France

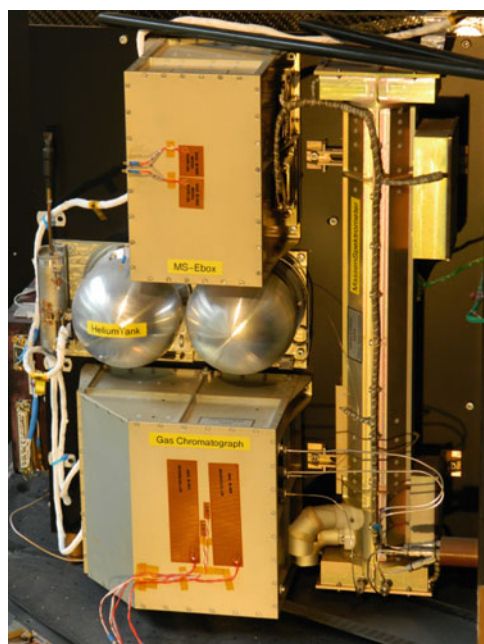


Fig. 13 The COSAC Experiment on the Philae Lander that will land on the nucleus of comet 67P/Churyumov-Gerasimenko. COSAC will receive cometary sample from the Sample Drill and Distribution System and analyze them for organic composition and homochirality. The image shows two helium tanks (each of volume 330 cm³); the gas chromatograph box at the *bottom* contains the GC hardware frame and its affiliate electronics; the MS-Ebox (electronic box) contains the affiliate electronics for the mass spectrometer. The TOFMS seen here is arranged vertically on the *right*. The flight instrument is protected from radiation and cometary debris by the solar panels of the Philae unit. The entire instrumental suite is 500 mm tall and 400 mm wide

adhere to the payload requisites. Helium will be used as a carrier gas in the GC component as it is chemically inert, has a higher thermal conductivity relative to many organic molecules, and is not likely to be found on the cometary nucleus. The

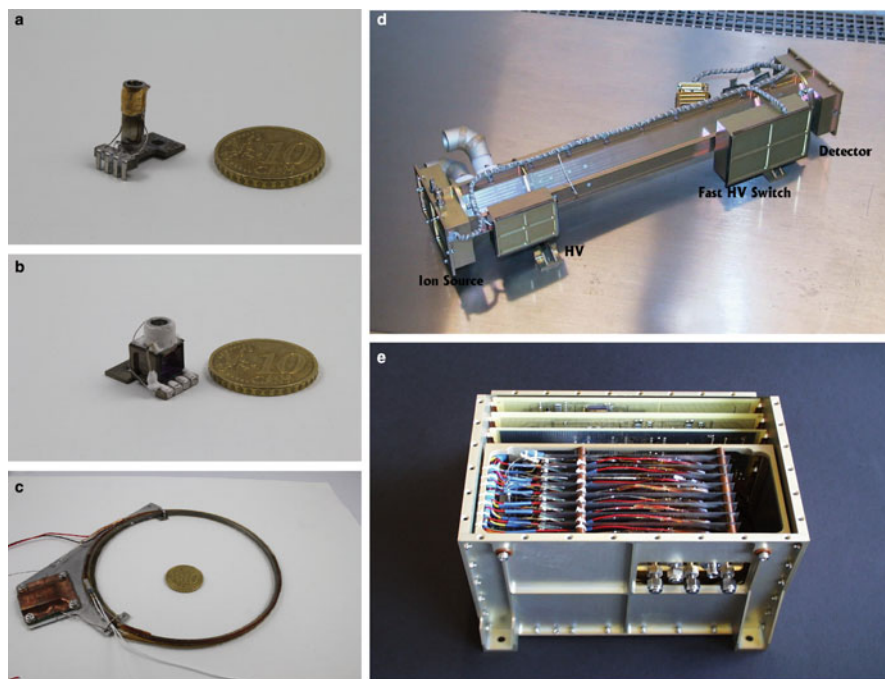


Fig. 14 (a) COSAC high temperature oven (heats up to 600°C). (b) COSAC medium temperature oven (heats up to 180°C). (c) Typical COSAC capillary chromatographic column arranged in a ring formation along with the thermal conductivity detector below the copper plate (inner diameter 100 mm). (d) COSAC time-of-flight mass spectrometer (460 mm long). (e) Pneumatic gas chromatography hardware mounting frame (80 mm width, 120 mm length, 105 mm height). The frame consists of eight different chromatographic columns and their respective TCDs connected to the incoming gas supply as well as the exhaust via thermally operated valves

carrier gas has been packed in two spherical tanks each of volume 330 cm³ that are filled to a pressure of 40 bar.

The calibration gas that will be used during the COSAC Experiment is a mixture of noble gases of the following composition: 24% Ne, Ar, Kr, Xe, and 4% He. The pressure regulation for the gas flow will be performed using thermally operated valves that run on the principle of thermal expansion. The thermally operated valve is a patented technology developed and produced at the Max Planck Institute for Solar System Research, Germany. The gas distribution system in the GC is controlled by 28 indigenously developed on-off switching valves. These valves work in the temperature range from −60°C to +200°C.

The COSAC–GC possesses two different types of pyrolysis ovens in which the samples will be vaporized (Fig. 14). The medium temperature oven heats the sample to 180°C and allows real-time sample monitoring in the visible and infrared region by CIVA through a window at the bottom of the oven. The other type of pyrolysis oven is the high temperature oven that can heat samples to 600°C without

Table 6 Chromatographic columns in the COSAC–GC

Column	Length (m)	Inner diameter (mm)	Stationary phase thickness(μm)
<i>Enantioselective columns</i>			
Chirasil L Val	12.5	0.25	0.12
Chirasil Dex CB	10	0.25	0.25
Cyclodextrin G-TA	10	0.25	0.125
<i>General columns</i>			
MXT 1	10	0.18	0.1
MXT 20	15	0.18	1.0
MXT 1701	15	0.18	1.2
MXT U-PLOT	10	0.18	1.0
CarboBond	15	0.25	10

any provision for real-time inspection [130]. The chromatographic columns and detectors are the analytical heart of the COSAC–GC (Fig. 14). There are a total of eight columns of varying stationary phase thicknesses, diameters, and lengths: five of these are standard GC columns aiming to separate substantially different molecules and the other three are enantioselective columns that will be used to detect chiral organic molecules (Table 6).

Each of these eight columns is fitted with a micro-machined thermal conductivity detector (TCD) manufactured by Varian. This TCD is in principle a Wheatstone bridge of four filaments that are supplied with a constant voltage and are cooled by two parallel, symmetrical, and opposite flows of gas. A signal is obtained when an analyte, which has a lower thermal conductivity relative to the carrier gas, enters the gas flow. This increases the temperature of the filament and, due to the temperature co-efficient of resistance of filament, this temperature change yields a differentiating output voltage.

The COSAC–TOFMS is a high-resolution multi-pass time-of-flight instrument. It can be used in either stand-alone or GC–TOFMS mode. The gas molecules entering the mass spectrometer will be ionized by a beam of electrons. These ionized molecules, depending on their m/z ratio, will travel towards a multi-sphere detector to produce a characteristic spectral signal.

At lower resolutions only a single-flight path, 370 mm distant from the source, will be used. For higher resolution runs, the TOFMS is to be used in multiple-turn mode, which is accomplished using two gridless reflectors, one near the source, the other on the opposite side of the source. The resolution of COSAC–MS is 200 and it can measure masses from 1 to 1,500 amu [131].

6.2 The Scientific Vision of COSAC

The GC–MS unit of the COSAC Experiment will be the first of its kind to conduct in situ compositional analysis of a cometary nucleus. Numerous interstellar ice simulation experiments and analyses of meteoritic samples have afforded many

Table 7 Organic molecules separated by the chirality module of COSAC

Enantioselective columns of COSAC	Directed chiral analytes
Chirasil Dex CB	Hydrocarbons
Chirasil-L-Val	Carboxylic acids; amino acids
Cyclodextrin G-TA	Alcohols; diols

theories about the mechanisms that afforded (and continue to afford) the delivery of exogenous material to Earth. These theories will be put to the test as COSAC explores the nucleus of Comet 67P.

Comets have been long considered “dirty icy bodies” due to their high organic and aqueous content. These adjectives were originally used based on data from ground-based observations of numerous cometary missions like Giotto, Stardust, and Deep Impact. The detection of the amino acid glycine from the strewn dust of comet 81P/Wild-2 by Stardust [132] supports the possibility of discovering larger organic molecules on Comet 67P; however it should be noted that all comets do not necessarily have similar chemical compositions. The orbit of a comet, its radiation dosage, the age of the comet in a particular orbit, its size, volume, and other physical factors all govern their respective compositions. Comet 67P will only provide initial data towards a more complete understanding of the chemical composition of comets.

The search for amino acids and other organic chiral molecules is of fundamental interest to the Rosetta mission. The COSAC experiment’s enantioselective columns were carefully selected to allow for resolution of simple enantiomers and to initiate potentially an understanding of the origin of biomolecular homochirality within the solar system [131, 133]. The use of different enantioselective chromatographic columns (Table 7) will ensure resolution of a wide range of chiral molecules that could be encountered, including amino acids, amines, diols, alcohols, hydroxy carboxylic acids, and hydrocarbons such as *R,S*-3-methylhexane and its higher homologues [134].

The polar nature of amino acids requires their derivatization in order to transform them into more volatile and less reactive analytes prior to gas chromatographic analysis. Bulky, non-polar silyl groups or different esterification methods are traditionally used to convert the polar functional groups on OH, NH₂, and SH into nonpolar moieties. These conventional methods cannot be used during the COSAC experiment: sample analysis will be conducted in vacuum, at low temperatures, and under low gravity, excluding any solvent chemistry. An alternative dry derivatization method using DMF–DMA has therefore been selected for the COSAC experiment [135]. This method entails simultaneously exposing the sample to pyrolysis and a suitable gas phase derivatization agent. Pyrolysis is preferred in this instance over the conventional procedure of acid hydrolysis because pyrolysis does not require wet chemistry and reduces the complexity of the experimental set-up. Capsules of DMF–DMA have been placed within the COSAC assembly in the pyrolysis oven, where they will melt and release DMF–DMA once temperatures of 100°C are reached within the oven-injector

system of the COSAC experiment [135]. Derivatized amino acids (and other small molecules) will then be resolvable on the GC module and can also be transferred into the mass spectrometer for identification via characteristic mass fragmentation analysis.

Within the first few hours of landing, the COSAC Experiment will first perform an initial set of experiments known as the first science sequence (FSS). This FSS will be powered by a set of on-board batteries. The long-term science phase (LTS) will be then be conducted until the end of the mission and these experiments will be powered by the solar panels on PHILAE. The data generated will be uplinked to the orbiter and then to Earth for analysis.

7 Outlook

There are numerous proposed mechanisms via which amino acids could have been generated in interstellar space. It is currently thought that the substrates supporting amino acid synthesis were likely to have been IDPs that could then have been incorporated into comets, asteroids, and planets. The likely mechanism of homochiral amino acid synthesis suggests photochemical triggering by circularly polarized photons that subsequently induced asymmetric amino acid formation on icy grains and comets. The presence of liquid water on comets or meteorites may have served to enhance amino acid production and homochirality via Strecker processes. At the same time, photochemistry may also have induced amino acid synthesis on icy grains and comets via chemistry involving radical mechanisms. It is likely that the COSAC experiment will provide some insight into which of these mechanisms might have afforded amino acid synthesis in interstellar contexts.

The science of the origin of life does not fall strictly into the domain of biology and chemistry – rather it is cross-disciplinary and involves additional fields such as astronomy, geology, and physics for a complete appreciation of how life in our universe may have come into existence. Thus the discoveries of the roles that carbon stars, supernovae, and any other astrophysical phenomena play in the creation of prebiotic molecules could significantly contribute to a scientific understanding of life's origins. Continued ice simulation experiments on Earth and meteorite analyses, combined with exploration missions into interstellar space, will likely yield further answers. The successful landing of ROSETTA on comet 67P/Churyumov-Gerasimenko in November 2014 will open a new chapter in the history of space exploration. This first attempt to detect large quantities of organic molecules in situ on a cometary nucleus will hopefully yield clues for the presence and diversity of prebiotic molecules and homochirality in the universe and further insight into the origin of life itself.

Acknowledgements We thank the generous support provided by the Max Planck Institute for Solar System Research, Deutsches Zentrum für Luft- und Raumfahrt, Centre National d'Etudes Spatiales, the RSC JWT Jones Fellowship (for A.C.E.), the European Space Agency, as well as the synchrotron centers SOLEIL, Gif-sur-Yvette, France, and the Institute for Storage Ring Facilities at Aarhus University, Denmark.

Author contributions: C.G., C.M., and A.C.E. wrote the manuscript. F.G. is the principal investigator of ROSETTA's COSAC instrument and led the writing of Sect. 6. U.J.M. initiated research programs on biomolecular asymmetry and defined major science subjects as written in Sects. 4 and 5.

References

1. Suess ST (1990) The heliosphere. *Rev Geophys* 28:97–115
2. Tielens AGGM (2005) The physics and chemistry of the interstellar medium. Cambridge University Press, Cambridge
3. Ferrière KM (2001) The interstellar environment of our galaxy. *Rev Mod Phys* 73:1031–1066
4. Spitzer L (1978) Physical processes in the interstellar medium. Wiley, New York
5. Morton DC, Drake JF, Jenkins EB, Rogerson JB, Spitzer L, York DG (1973) Spectrophotometric results from the Copernicus satellite II. Composition of interstellar clouds. *Astrophys J* 181:103–109
6. Savage BD, Sembach KR (1996) Interstellar abundances from absorption-line observations with the Hubble Space Telescope. *Annu Rev Astron Astrophys* 34:279–329
7. Field GB, Somerville WB, Dressler K (1966) Hydrogen molecules in astronomy. *Annu Rev Astron Astrophys* 4:207–244
8. Sanders DB, Scoville NZ (1991) Molecular gas in luminous infrared galaxies. *Astrophys J* 370:158–171
9. Wilson RW, Jefferts KB, Penzias AA (1970) Carbon monoxide in the Orion nebula. *Astrophys J* 161:43–44
10. Irvine WM (1991) The molecular composition of dense interstellar clouds. In: Greenberg JM, Pirronello V (eds) Chemistry in space – NATO ASI Series C 323:89–121
11. Herbst E, van Dishoeck EF (2009) Complex organic interstellar molecules. *Annu Rev Astron Astrophys* 47:427–480
12. Meierhenrich UJ, Filippi J-J, Meinert C, Vierling P, Dworkin JP (2010) On the origin of primitive cells: from nutrient intake to elongation of encapsulated nucleotides. *Angew Chem Int Ed* 49:3738–3750
13. Meierhenrich UJ, Filippi J-J, Meinert C, Vierling P, Dworkin JP (2010) Die Entstehung erster Zellen – von der Nährstoffaufnahme hin zur Verlängerung eingeschlossener Nucleotide. *Angew Chem* 122:3826–3839
14. Suess HE, Urey HC (1956) Abundances of the elements. *Rev Mod Phys* 28:53–74
15. Castor JI, Abbott DC, Klein RI (1975) Radiation-driven winds in Of stars. *Astrophys J* 195:157–174
16. Loup C, Forveille T, Omont A, Paul JF (1993) CO and HCN observations of circumstellar envelopes. A catalogue – mass loss rates and distributions. *Astron Astrophys Suppl Ser* 99:291–377
17. Cernicharo J, Goicoechea JR, Caux E (2000) Far-infrared detection of C₃ in Sagittarius B2 and IRC +10216. *Astrophys J* 534:199–202
18. Becklin EE (1969) The unusual infrared object IRC +10216. *Astrophys J* 158:133–137
19. Gilman RC (1969) On the composition of circumstellar grains. *Astrophys J* 159:185–187
20. Sahai R, Chronopoulos CK (2010) The astrosphere of asymptotic giant branch star IRC +10216. *Astrophys J* 711:53–56

21. Ehrenfreund P, Charnley SB (2000) Organic molecules in the interstellar medium, comets, and meteorites: a voyage from dark clouds to the early Earth. *Annu Rev Astron Astrophys* 38:427–483
22. De Beck E, Lombaert R, Agúndez M, Daniel F, Decin L, Cernicharo J, Müller HSP, Min M, Royer P, Vandenbussche B, de Koter A, Waters LBFM, Groenewegen MAT, Barlow MJ, Guélin M, Kahane C, Pearson JC, Encrenaz P, Szczerba R, Schmidt MR (2012) On the physical structure of IRC +10216 – ground-based and Herschel observations of CO and C₂H. <http://arxiv.org/pdf/1201.1850.pdf>. Accessed 9 Mar 2012
23. Gustaffson B (2010) Astrophysics: unexpected warm water. *Nature* 467:35–36
24. Tielens AGGM, Charnley SB (1997) Circumstellar and interstellar synthesis of organic molecules. In: Whittet DCB (ed) *Origins of life evolution of the biosphere*. Kluwer Academic, Dordrecht
25. Bell MB, Avery LW, MacLeod JM, Matthews HE (1992) The excitation temperature of HC₉N in the circumstellar envelope of IRC +10216. *Astrophys J* 400:551–555
26. Cernicharo J, Guélin M (1996) Discovery of C₈H radical. *Astron Astrophys* 309:27–30
27. Langer WD, Velusamy T, Kuiper TB, Peng R, McCarthy MC, Travers MJ, Kovács A, Gottlieb CA, Thaddeus P (1997) First astronomical detection of the cumulene carbon chain molecule H₂C₆ in TMC-1. *Astrophys J* 480:63–66
28. Guélin M, Cernicharo J, Travers MJ, McCarthy MC, Gottlieb CA, Thaddeus P, Ohishi M, Saito S, Yamamoto S (1997) Detection of a new linear carbon chain radical: C₇H. *Astron Astrophys* 317:1–4
29. Spaans M, Ehrenfreund P (1999) In: Ehrenfreund P, Krafft C, Kochan H, Pirronello V (eds) *Laboratory astrophysics and space research*. Kluwer Academic, Dordrecht
30. Evans NJ II (1999) Physical conditions in regions of star formation. *Annu Rev Astron Astrophys* 37:311–362
31. Greenberg JM (1986) The role of grains in molecular chemical evolution. *Astrophys Space Sci* 128:17–31
32. Herbst E (1987) In: Hollenbach DJ, Thronson HA (eds) *Interstellar processes*. Riedel, Dordrecht
33. Millar TJ, Hatchell J (1998) Chemical models of hot molecular cores. *Faraday Discuss* 109:15–30
34. Trumpler RJ (1930) Absorption of light in the galactic system. *Publ Astron Soc Pac* 42:214–227
35. Jones AP, Tielens AGGM (1994) In: Montmorle T, Lada CJ, Mirabel IF, Tran Than Van J (eds) *The cold universe*. Editions Frontières, Gif-sur-Yvette
36. Henning T (1999) Grain formation and evolution in the interstellar medium. In: Le Seargent d'Hendecourt L, Joblin C, Jones A (eds) *Solid interstellar matter: the ISO revolution*. EDP Science/Springer, Les Ulis/Heidelberg
37. Dunne L, Eales S, Ivison R, Morgan H, Edmunds M (2003) Type II supernovae as a significant source of interstellar dust. *Nature* 424:285–287
38. Morgan HL, Edmunds MG (2003) Dust formation in early galaxies. *Mon Not R Astron Soc* 343:427–442
39. Sandford SA, Allamandola LJ (1993) H₂ in interstellar and extragalactic ices: infrared characteristics, ultraviolet production, and implications. *Astrophys J* 409:65–68
40. Greenberg JM (1978) Interstellar dust. In: McDonnell JAM (ed) *Cosmic dust*. Wiley-Interscience, New York
41. Charnley SB, Rogers SD, Ehrenfreund P (2001) Gas-grain chemical models of star forming molecular clouds as constrained by ISO and SWAS observations. *Astron Astrophys* 378:1024–1036
42. Allamandola LJ, Sandford SA, Tielens AGGM, Herbst TM (1992) Infrared spectroscopy of dense clouds in the C-H stretch region: methanol and “diamonds”. *Astrophys J* 399:134–146
43. Boogert ACA, Ehrenfreund P, Gerakines PA, Tielens AGGM, Whittet DCB, Schutte WA, van Dishoeck EF, de Graauw T, Decin L, Prusti T (2000) ISO-SWS observations of

- interstellar solid $^{13}\text{CO}_2$: heated ice and the galactic $^{12}\text{C}/^{13}\text{C}$ abundance ratio. *Astron Astrophys* 353:349–362
44. de Graauw T, Whittet DCB, Gerakines PA, Bauer OH, Beintema DA, Boogert ACA, Boxhoom DR, Chiar JE, Ehrenfreund P, Feuchtgruber H, Helmich FP, Heras AM, Huygen R, Kester DJM, Kunze D, Lahuis F, Leech KJ, Lutz D, Morris PW, Prusti T, Roelfsema PR, Salama A, Schaeidt SG, Schutte WA, Spoon HWW, Tielens AGGM, Valentijn EA, Vandenbusshe B, van Dishoeck EF, Wesselius PR, Wieprecht E, Wright CM (1996) SWS observations of solid CO_2 in molecular clouds. *Astron Astrophys* 315:345–348
 45. Ohishi M, Irvine WM, Kaifu N (1992) In: Singh PD (ed) *Astrochemistry of cosmic phenomena*. Kluwer, Dordrecht
 46. Nummelin A, Whittet DCB, Gibb EL, Gerakines PA (2001) Solid carbon dioxide in regions of low mass star formation. *Astrophys J* 558:185–193
 47. Blake GA, Sutton EC, Masson CR, Phillips TG (1987) Molecular abundances in OMC-1 – the chemical composition of interstellar molecular clouds and the influence of massive star formation. *Astrophys J* 315:621–645
 48. Le Sergeant d’Hendecourt L, Allamandola LJ, Greenberg JM (1985) Time dependent chemistry in dense molecular clouds I. Grain surface reactions, gas/grain interactions and infrared spectroscopy. *Astron Astrophys* 152:130–150
 49. Garrod RT, Weaver SLW, Herbst E (2008) Complex chemistry in star-forming regions: an expanded gas-grain warm-up chemical model. *Astrophys J* 682:283–302
 50. Millar TJ (2001) Molecules in high-mass star-forming regions – theory and observation. *Astron Soc Pac Conf Ser* 235:45–58
 51. Duley WW (2000) Chemical evolution of carbonaceous material in interstellar clouds. *Astrophys J* 528:841–848
 52. Mason NJ, Dawes A, Holtom PD, Mukerji RJ, Davis MP, Sivaraman B, Kaiser RI, Hoffman SV, Shaw DA (2006) VUV spectroscopy and photo-processing of astrochemical ices: an experimental study. *Faraday Discuss* 133:311–329
 53. Laffon C, Lacombe S, Bournel F, Parent P (2006) Radiation effects in water ice: a near edge X-ray absorption fine structure study. *J Chem Phys* 125:204714
 54. Muñoz Caro GM, Jiménez-Escobar A, Martín-Gago JA, Rogero C, Atienza C, Puertas S, Sobrado JM, Torres-Redondo J (2010) New results on thermal and photodesorption of CO ice using the novel InterStellar Astrochemistry Chamber (ISAC). *Astron Astrophys* 522:108–122
 55. Ciaravella A, Jiménez-Escobar A, Muñoz Caro GM, Cecchi-Pestellini C, Candia R, Giarrusso S, Barbera M, Collura A (2012) Soft X-ray irradiation of pure carbon monoxide interstellar ice analogues. *Astrophys J Lett* 746:L1
 56. Ehrenfreund P, Fraser H (2003) Ice chemistry in space. In: Pirronello V, Krelowski J, Manicò G (eds) *Proceedings of the NATO advanced study institute on solid state astrochemistry*, Kluwer Academic, Dordrecht
 57. Schutte WA (1999) Ice evolution in the interstellar medium. In: Le Sergeant d’Hendecourt L, Joblin C, Jones A (eds) *Solid interstellar matter: the ISO revolution*. EDP Science/Springer, Les Ulis/Heidelberg
 58. Hegstrom RA, Rein DW, Sandars PGH (1979) Parity non-conserving energy difference between mirror-image molecules. *Phys Lett A* 71:499–502
 59. Yamagata Y (1966) A hypothesis for the asymmetric appearance of biomolecules on Earth. *J Theor Biol* 11(3):495–498
 60. Mason S, Tranter G (1984) The parity violating energy difference between enantiomeric molecules. *Mol Phys* 53:1091–1111
 61. Tranter G (1987) Parity violation and the origins of biomolecular handedness. *Biosystems* 20:37–48
 62. Tranter GE, McDermott AJ (1989) Electroweak bioenantioselection. *Chem Phys Lett* 163:1–4
 63. Berger R, Quack M (2000) Electroweak quantum chemistry of alanine: parity violation in gas and condensed phases. *ChemPlusChem* 1:57–60

64. Laerdahl JK, Wesendrup R, Schwerdtfeger P (2000) D- or L-alanine: that is the question. *Chemphyschem* 1:60–62
65. Rosenberg RA (2011) Spin-polarized e-induced asymmetric reactions in chiral molecules. *Top Curr Chem* 298:279–306
66. Bonner WA, Van Dort MA, Yearian MR (1975) Asymmetric degradation of DL-leucine with longitudinally polarized electrons. *Nature* 258:419–421
67. Ulbricht TLV, Vester F (1962) Attempts to induce optical activity with polarized beta radiation. *Tetrahedron* 18:629–637
68. Bonner WA, Flores JJ (1975) Experiments on the origins of optical activity. *Orig Life Evol Biosph* 6:187–194
69. Inoue Y (1992) Asymmetric photochemical reactions in solution. *Chem Rev* 92:741–770
70. Buchard O (1974) Photochemistry with circularly polarized light. *Angew Chem Int Ed Engl* 13:179–185
71. Rau H (1983) Asymmetric photochemistry in solution. *Chem Rev* 83:535–547
72. Kuhn W, Braun E (1929) Photochemical preparation of optically active substances. *Naturwissenschaften* 17:227–228
73. Kuhn W, Knopf E (1930) The preparation of optically active compounds by the aid of light. *Z Phys Chem* 7:292–310
74. Flores JJ, Bonner WA, Massey GA (1977) Asymmetric photolysis of (RS)-leucine with circularly polarized ultraviolet light. *J Am Chem Soc* 99:3622–3625
75. Balavoine G, Moradpour A, Kagan HB (1974) Preparation of chiral compounds with high optical purity by irradiation with circularly polarized light, a model reaction for the prebiotic generation of optical activity. *J Am Chem Soc* 96:5152–5158
76. Norden B (1997) Was photoresolution of amino acids the origin of optical activity of life? *Nature* 266:567–568
77. Nishino H, Kosaka A, Hembury GA, Shitomi H, Onuki H, Inoue Y (2001) Mechanism of pH-dependent photolysis of aliphatic amino acids and enantiomeric enrichment of racemic leucine by circularly polarized light. *Org Lett* 3:921–924
78. Meierhenrich UJ, Nahon L, Alcaraz C, Bredehöft JH, Hoffmann SZ, Barbier B, Brack A (2005) Asymmetric vacuum UV photolysis of the amino acid leucine in the solid state. *Angew Chem Int Ed* 44:5630–5634
79. Meierhenrich UJ, Nahon L, Alcaraz C, Bredehöft JH, Hoffmann SZ, Barbier B, Brack A (2005) Asymmetrische Vakuum-UV Photolyse der Aminosäure Leucin in fester Phase. *Angew Chem* 117:5774–5779
80. Bailey J (2001) Astronomical sources of circularly polarized light and the origin of homochirality. *Orig Life Evol Biosph* 31:167–183
81. Bailey J, Chrysostomou A, Hough JH, Gledhill TM, McCall A, Clark S, Ménard F, Tamura M (1998) Circular polarization in star-formation regions: implications for biomolecular homochirality. *Science* 281:672–674
82. Buschermöhle M, Whittet DCB et al (2005) An extended search for circularly polarized infrared radiation from the OMC-1 region of Orion. *Astrophys J* 624:821–826
83. Fukue T, MetM T et al (2009) Near-infrared circular polarimetry and correlation diagrams in the Orion Becklin-Neugebauer/Kleinman-low region: contribution of dichroic extinction. *Astrophys J* 692:88–91
84. Minchin NR, Hough JH, Burton MG, Yamashita T (1991) Near-infrared imaging polarimetry of bipolar nebulae – IV. GL490, GL 2789 and GL 2136. *Mon Not R Astron Soc* 251:522–528
85. Lucas PW, Hough JH, Bailey J, Chrysostomou A, Gledhill TM, McCall A (2005) UV circular polarisation in star formation regions: the origin of homochirality? *Orig Life Evol Biosph* 35:29–60
86. Svensmark H (2012) Evidence of nearby supernovae affecting life on Earth. *Mon Not R Astron Soc* 423:1234–1253
87. Diehl R, Halloin H, Kretschmer K et al (2006) Radioactive ^{26}Al from massive stars in the galaxy. *Nature* 439:45–47

88. Sandford SA, Aléon J et al (2006) Organics captured from comet 81P/Wild 2 by the Stardust Spacecraft. *Science* 314:1720–1724
89. Oro J, Gibert J, Lichtenstein H, Wikstrom S, Flory DA (1971) Amino-acids, aliphatic and aromatic hydrocarbons in the Murchison meteorite. *Nature* 230:105–106
90. Robert F, Epstein S (1982) The concentration and isotopic composition of hydrogen, carbon and nitrogen in carbonaceous meteorites. *Geochim Cosmochim Acta* 46:81–95
91. Kvenvolden KA, Lawless JG, Ponnamperna C (1971) Non-protein amino acids in the Murchison meteorite. *Proc Natl Acad Sci USA* 68:486–490
92. Cronin JR, Pizzarello S (1997) Enantiomeric excesses in meteoritic amino acids. *Science* 275:951–955
93. Pizzarello S, Cronin JR (2000) Non-racemic amino acids in the Murray and Murchison meteorites. *Geochim Cosmochim Acta* 64:329–338
94. Glavin DP, Dworkin JP (2009) Enrichment of the amino acids L-isovaline by aqueous alteration on CI and CM meteorite parent bodies. *Proc Natl Acad Sci* 106:5487–5492
95. Muñoz Caro GM, Meierhenrich UJ, Schutte WA, Barbier B, Arcones Segovia A, Rosenbauer H, Thiemann WH-P, Brack A, Greenberg JM (2002) Amino acids from ultraviolet irradiation of interstellar ice analogues. *Nature* 416:403–406
96. Bernstein MP, Dworkin JP, Sandford SA, Cooper GW, Allamandola LJ (2002) Racemic amino acids from the ultraviolet photolysis of interstellar ice analogues. *Nature* 416:401–403
97. Holtom PD, Bennett CJ, Osamura Y, Mason NJ, Kaiser RI (2005) A combined experimental and theoretical study on the formation of the amino acid glycine ($\text{NH}_2\text{CH}_2\text{COOH}$) and its isomer (CH_3NHCOOH) in extraterrestrial ices. *Astrophys J* 626:940–952
98. Briggs R, Ertem G, Ferris JP, Greenberg JM, McCain PJ, Mendoza-Gomez CX, Schutte W (1992) Comet Halley as an aggregate of interstellar dust and further evidence for the photochemical formation of organics in the interstellar medium. *Orig Life Evol Biosph* 22:287–307
99. d'Hendecourt LB, Allamandola LJ, Baas F, Greenberg JM (1982) Inter-stellar grain explosions – molecule cycling between gas and dust. *Astron Astrophys* 109:12–14
100. Meinert C, Filippi J-J, de Marcellus P, Seargent L, d'Hendecourt L, Meierhenrich UJ (2012) *N*-(2-Aminoethyl)glycine and amino acids from interstellar ice analogues. *Chempluschem* 77:186–191
101. Nahon L, de Oliveira N, Garcia G, Gil JF, Pilette B, Marcouille O, Lagarde B, Polack F (2012) DESIRS: a state-of-the-art VUV beamline featuring high resolution and variable polarization for spectroscopy and dichroism at SOLEIL. *J Synchrotron Radiat* 19:508–520
102. Nahon L, Alcaraz C (2004) SU5: a calibrated variable-polarization synchrotron radiation beam line in the vacuum-ultraviolet range. *Appl Opt* 43:1024–1037
103. Meierhenrich UJ (2008) Amino acids and the asymmetry of life – caught in the act of formation. Springer, Heidelberg
104. Meierhenrich UJ, Muñoz Caro GM, Bredehöft JH, Jessberger EK, Thiemann WH-P (2004) Identification of diamino acids in the Murchison meteorite. *Proc Natl Acad Sci USA* 101:9182–9186
105. Meierhenrich UJ, Filippi J-J, Meinert C, Bredehöft JH, Takahashi J, Nahon L, Jones NC, Hoffmann SV (2010) Circular dichroism of amino acids in the vacuum-ultraviolet region. *Angew Chem Int Ed* 49:7799–7802
106. Meierhenrich UJ, Filippi J-J, Meinert C, Bredehöft JH, Takahashi J, Nahon L, Jones NC, Hoffmann SV (2010) Circular dichroismus von Aminosäuren im Vakuum-Ultraviolett. *Angew Chem* 122:7966–7970
107. Adrian-Scotto M, Antonczak S, Bredehöft JH, Hoffmann SV, Meierhenrich UJ (2010) Chiroptical properties of amino acids: a density functional theory study. *Symmetry* 2:935–949
108. Meierhenrich UJ, Filippi J-J, Meinert C, Hoffmann SV, Bredehöft JH, Nahon L (2010) Photolysis of rac-Leucine with circularly polarized synchrotron radiation. *Chem Biodivers* 7:1651–1659

109. Meierhenrich UJ, Filippi J-J, Meinert C, Hoffmann SV, Bredehöft JH, Nahon L (2011) Photolysis of rac-leucine with circularly polarized synchrotron radiation. In: Brückner H, Fujii N (eds) *D-Amino acids in chemistry, life sciences, and biotechnology*. Wiley-VCH, Weinheim
110. Evans AC, Meinert C, Giri C, Goesmann F, Meierhenrich UJ (2012) Chirality, photochemistry and the detection of amino acids in interstellar ice analogues and comets. *Chem Soc Rev* 41:5447–5458
111. Frank FC (1953) On spontaneous asymmetric synthesis. *Biochim Biophys Acta* 11:459–463
112. Kondepudi DK, Prigogine I (1998) *Modern thermodynamics: from heat engines to dissipative structures*. Wiley, New York
113. Kondepudi DK, Asakura K (2001) Chiral autocatalysis, spontaneous symmetry breaking, and stochastic behavior. *Acc Chem Res* 34:946–954
114. Soai K, Shibata T, Morioka H, Choji K (1995) Asymmetric autocatalysis and amplification of enantiomeric excess of a chiral molecule. *Nature* 378:767–768
115. Breslow R, Levine M (2006) Amplification of enantiomeric concentrations under credible prebiotic conditions. *Proc Natl Acad Sci USA* 103:12979–12980
116. Klussmann M, Iamura H, Mathew S, Wells D, Pandya U, Armstrong A, Blackmond D (2006) Thermodynamic control of asymmetric amplification in amino acid catalysis. *Nature* 441:621–623
117. Noorduyn W, Izumi T, Millemaggi A, Leeman M, Meekes H, Van Enckevort W, Kellogg R, Kaptein B, Vlieg E, Blackmond D (2008) Emergence of single solid chiral state from a nearly racemic amino acid derivative. *J Am Chem Soc* 130:1158–1159
118. Viedma C, Ortiz J, de Torres T, Izumi T, Blackmond D (2008) Evolution of solid phase homochirality for a proteinogenic amino acid. *J Am Chem Soc* 130:15274–15275
119. Nielsen PE (1993) Peptide nucleic-acid (PNA) – a model structure for the primordial genetic material. *Orig Life Evol Biosph* 123:323–327
120. Muñoz Caro GM, Meierhenrich UJ, Schutte WA, Greenberg JM, Thiemann W (2004) UV-photoprocessing of interstellar ice analogs: detection of hexamethylenetetramine-based species. *Astron Astrophys* 413:209–216
121. Meierhenrich UJ, Muñoz Caro GM, Schutte WA, Thiemann WH-P, Barbier B, Brack A (2005) Precursors of biological cofactors from ultraviolet irradiation of circumstellar/interstellar ice analogs. *Chemistry* 11:4895–4900
122. Nuevo M, Bredehöft JH, Meierhenrich UJ, d’Hendecourt L, Thiemann WH-P (2010) Urea, glycolic acid, and glycerol in an organic residue produced by ultraviolet irradiation of interstellar/precometary ice analogs. *Astrobiology* 10:245–256
123. Bonnet RM (1985) The new mandatory scientific programme for ESA. *ESA Bull* 43:8–13
124. Huber MCE, Schwehm G (1991) Comet nucleus sample return: plans and capabilities. *Space Sci Rev* 56:109–115
125. Schwehm G, Schulz R (1999) ROSETTA goes to comet Wirtanen. *Space Sci Rev* 90:313–319
126. Weismann PR, Asphaug E, Lowry SC (2004) Structure and density of cometary nuclei. In: Festou MC, Keller HU, Weaver HA (eds) *Comets II*. University of Arizona Press, Tucson
127. Glassmeier K-H, Boehnhardt H, Koschny D, Kührt E, Richter I (2008) The ROSETTA mission: flying towards the origin of the solar system. In: Schulz R, Alexander C, Boehnhardt H, Glassmeier K-H (eds) *ROSETTA ESA’s mission to the origin of the solar system*. Springer, New York
128. Bibring J-P, Rosenbauer H, Boehnhardt H, Ulamec S, Biele J, Espinasse S, Feuerbacher B, Gaudon P, Hemmerich P, Klestzki P et al (2007) The ROSETTA lander (“PHILAE”) investigations. *Space Sci Rev* 128:205–220
129. Goesmann F, Rosenbauer H, Roll R, Boehnhardt H (2005) COSAC onboard Rosetta: a bioastronomy experiment for the short-period comet 67P/Churyumov-Gerasimenko. *Astrobiology* 5:622–631

130. Goesmann F, Rosenbauer H, Roll R, Szopa C, Raulin F, Sternberg R, Israel G, Meierhenrich UJ, Thiemann W, Muñoz Caro GM (2007) COSAC, the cometary sampling and composition experiment on PHILAE. *Space Sci Rev* 128:257–280
131. Meierhenrich U, Thiemann WH-P, Rosenbauer H (1999) Molecular parity violation via comets? *Chirality* 11:575–582
132. Elsila JE, Glavin DP, Dworkin JP (2009) Cometary glycine detected in samples returned by Stardust. *Meteorit Planet Sci* 44:1323–1330
133. Thiemann WH-P, Rosenbauer H, Meierhenrich UJ (2001) Conception of the ‘chirality-experiment’ on ESA’s mission ROSETTA to comet 46P/Wirtanen. *Adv Space Res* 27:323–328
134. Meierhenrich UJ, Thiemann WH-P, Goesmann F, Roll R, Rosenbauer H (2001) Enantiomer separation of hydrocarbons in preparation of Rosetta’s ‘chirality-experiment’. *Chirality* 13:454–457
135. Meierhenrich U, Thiemann WH-P, Rosenbauer H (2001) Pyrolytic methylation assisted enantioseparation of chiral hydroxycarboxylic acids. *J Anal Appl Pyrolysis* 60:13–26

Biochirality

Origins, Evolution and Molecular Recognition

Cintas, P. (Ed.)

2013, VIII, 316 p., Hardcover

ISBN: 978-3-642-37625-2